

1 **Smaller global and regional carbon emissions from gross land use change when considering sub-**  
2 **grid secondary land cohorts in a global dynamic vegetation model**

3  
4 Chao Yue, Philippe Ciais, Wei Li

5  
6 Laboratoire des Sciences du Climat et de l'Environnement, LSCE/IPSL, CEA-CNRS-UVSQ, Université  
7 Paris-Saclay, F-91191 Gif-sur-Yvette, France

8  
9 Corresponding author: Chao Yue, [chao.yue@lsce.ipsl.fr](mailto:chao.yue@lsce.ipsl.fr)

10  
11 Running title: Land use carbon emissions with sub-grid land cohorts

12  
13 **Abstract**

14 Several modeling studies reported elevated carbon emissions from historical land use change ( $E_{LUC}$ ) by  
15 including bi-directional transitions on the sub-grid scale (termed gross land use change), dominated by  
16 shifting cultivation and other land turnover processes. However, most dynamic global vegetation models  
17 (DGVM) having implemented gross land use change either do not account for sub-grid secondary lands,  
18 or often have only one single secondary land tile over a model grid cell and thus cannot account for  
19 various rotation lengths in shifting cultivation and associated secondary forest age dynamics. Therefore it  
20 remains uncertain how realistic the past  $E_{LUC}$  estimations are and how estimated  $E_{LUC}$  will differ between  
21 the two modeling approaches with and without multiple sub-grid secondary land cohorts — in particular  
22 secondary forest cohorts. Here we investigated historical  $E_{LUC}$  over 1501–2005 by including sub-grid  
23 forest age dynamics in a DGVM. We run two simulations, one with no secondary forests ( $S_{ageless}$ ) and the  
24 other with sub-grid secondary forests of 6 age classes whose demography is driven by historical land use  
25 change ( $S_{age}$ ). Estimated global  $E_{LUC}$  for 1501–2005 are 176 Pg C in  $S_{age}$  compared to 197 Pg C in  $S_{ageless}$ .  
26 The lower  $E_{LUC}$  in  $S_{age}$  arise mainly from shifting cultivation in the tropics under an assumed constant  
27 rotation length of 15 years, being of 27 Pg C in  $S_{age}$  in contrast to 46 Pg C in  $S_{ageless}$ . Estimated cumulative  
28  $E_{LUC}$  from wood harvest in the  $S_{age}$  simulation (31 Pg C) are however slightly higher than  $S_{ageless}$  (27 Pg C)  
29 when the model is forced by reconstructed harvested areas, because secondary forests targeted in  $S_{age}$  for  
30 harvest priority are insufficient to meet the prescribed harvest area, leading to wood harvest being  
31 dominated by old primary forests. An alternative approach to quantify wood harvest  $E_{LUC}$ , i.e., always  
32 harvesting the close-to-mature forests in both  $S_{ageless}$  and  $S_{age}$ , yields similar values of 33 Pg C by both  
33 simulations. The lower  $E_{LUC}$  from shifting cultivation in  $S_{age}$  simulations depends on the pre-defined  
34 forest clearing priority rules in the model and the assumed rotation length. A set of sensitivity model runs

35 over Africa reveal that a longer rotation length over historical period likely results in higher emissions.  
36 Our results highlight that although gross land use change as a former missing emission component is  
37 included by a growing number of DGVMs, its contribution to overall  $E_{LUC}$  remains uncertain and tends to  
38 be overestimated when models ignore sub-grid secondary forests.

39

40 Keywords: gross land use change, carbon emission, secondary forests, shifting cultivation, wood harvest.

41

## 42 **Nomenclature**

43 LUC : land use change

44  $E_{LUC}$  : carbon emissions from land use change. Positive values indicate that LUC has a net effect of  
45 releasing carbon from land to the atmosphere, while a negative value indicates the reverse.

46  $E_{LUC\ process[, configuration]}$  : carbon emissions from a certain LUC *process* (**net transitions only, land turnover,**  
47 **wood harvest** or **all three processes combined**) quantified by a specific model *configuration* (**age** or  
48 **ageless**, in which differently aged sub-grid land cohorts are, or are not explicitly represented,  
49 respectively). For instance,  $E_{LUC\ net, ageless}$  indicates  $E_{LUC}$  from net transitions only and without explicitly  
50 representing sub-grid age dynamics, i.e., a single ageless mature patch is used to represent a land cover  
51 type;  $E_{LUC\ net, age}$  indicates  $E_{LUC}$  from the same process using a model configuration that explicitly  
52 represents differently aged land cohorts.

53  $S_{age}$ : Model simulations that represents sub-grid secondary land cohorts.

54  $S_{ageless}$ : Model simulations that do not include sub-grid age dynamics, i.e., a single ageless mature patch is  
55 used to represent a land cover type.

56

## 57 **1 Introduction**

58 Historical land use change (LUC), such as the permanent establishment of agricultural land on forests  
59 (deforestation), shifting cultivation and wood harvest, has contributed significantly to the atmospheric  
60 CO<sub>2</sub> increase, in particular since industrialization (Houghton, 2003; Le Quéré et al., 2016; Pongratz et al.,  
61 2009). Carbon emissions from land use change ( $E_{LUC}$ ) are often defined as the net effect between carbon  
62 release on newly disturbed lands, given that in most cases newly created lands have a lower carbon  
63 density than natural ecosystems (e.g., deforestation or forest degradation), and carbon uptake on  
64 recovering ecosystems (e.g., cropland abandonment or afforestation/reforestation). As the high spatial  
65 heterogeneity of land conversions precludes any direct measurements of global or regional  $E_{LUC}$ ,  
66 modeling turned out to be the only approach to its quantification (Gasser and Ciais, 2013; Hansis et al.,  
67 2015; Houghton, 1999, 2003; Piao et al., 2009b). Methods to quantify  $E_{LUC}$  could fall broadly into three  
68 categories, namely bookkeeping models (Gasser and Ciais, 2013; Hansis et al., 2015; Houghton, 2003),

69 dynamic global vegetation models (Shevliakova et al., 2009; Stocker et al., 2014; Wilkenskjeld et al.,  
70 2014; Yang et al., 2010), and satellite-based estimates of deforestation fluxes (Baccini et al., 2012; van  
71 der Werf et al., 2010).

72  
73 When including sub-grid bi-directional gross land use changes such as shifting cultivation or other forms  
74 of land turnover processes, models are found to yield higher estimates of  $E_{LUC}$  for 1850-2005 by 2-38%  
75 than accounting for net transitions only (Hansis et al., 2015). Wood harvest, although it does not change  
76 the underlying land use type, can also lead to additional carbon emissions due to fast carbon release from  
77 recently harvested forests and slow uptake from re-growing ones (Shevliakova et al., 2009; Stocker et al.,  
78 2014). Because of their importance in estimating historical LUC emissions, gross land use change and  
79 wood harvest have been implemented in several dynamic global vegetation models (DGVMs), as  
80 synthesized in the Table 1 of Yue et al. (2017). A recent synthesis study by Arneeth et al. (2017) reported  
81 consistent increase in  $E_{LUC}$  by several models when including shifting cultivation and wood harvest, as  
82 well as other agricultural management processes such as pasture harvest and cropland management. These  
83 processes altogether yield an upward shift in estimated historical  $E_{LUC}$ , implying a larger potential in the  
84 land-based mitigation in the future if deforestation or forest degradation can be stopped.

85  
86 While replacing forest with cropland or pasture typically leads to carbon release, afforestation and forest  
87 regrowth following harvest or agricultural abandonment sequester carbon in growing biomass stocks.  
88 Some recent studies, on both site (Poorter et al., 2016) and regional scales (Chazdon et al., 2016), show  
89 that secondary forests recovering from historical LUC are contributing to the terrestrial carbon uptake,  
90 and that the carbon stored per unit land sometimes exceeds that of primary forests (Poorter et al., 2016).  
91 While explicit representation of sub-grid secondary forests and other lands with different years since the  
92 last disturbance (defined as cohorts or age classes) is straightforward in bookkeeping models (Hansis et  
93 al., 2015), and is fairly easy in some DGVMs combined with a forest gap model (e.g., LPJ-GUESS,  
94 Bayer et al., 2017), only a few DGVMs following an “area-based” approach (Smith et al., 2001) have  
95 done this but usually with a single secondary cohort for a given vegetation type (Yue et al., 2017).  
96 Shevliakova et al. (2009) pioneered the inclusion of both gross land use change and secondary lands in a  
97 DGVM. Their model can contain up to a total number of 12 secondary land cohorts, but the spatial  
98 separation of natural plant functional types (PFTs) was limited. In some other DGVMs (Kato et al., 2013;  
99 Stocker et al., 2014; Yang et al., 2010), secondary lands were limited to have one cohort per PFT. This  
100 has limited the accurate representation of the carbon balance in differently aged secondary forests.

101

102 In reality, shifting cultivation and wood harvest (forestry) tend to have certain rotation lengths (McGrath  
103 et al., 2015; van Vliet et al., 2012), which vary among different regions and management systems.  
104 Simulating these LUC activities by targeting forests with an appropriate age can have important  
105 consequences in derived  $E_{LUC}$ , since young versus old forests have very different aboveground biomass  
106 stocks. Using a bookkeeping model, Hansis et al. (2015) showed that assuming only secondary land  
107 clearing in gross change yields a 2% increase in  $E_{LUC}$  compared with accounting for net transitions only,  
108 much smaller than the 24% increase when assuming primary land clearing as a priority in gross change.  
109 The worldwide, systematic information on historical and present rotation lengths of shifting cultivation  
110 and wood harvest is missing. Some LUC reconstructions, such as the land-use harmonization version 1  
111 (LUH1) data (Hurtt et al., 2011), assumed a fixed rotation length of 15 years for shifting agriculture in the  
112 tropics, and this assumption has been used in some modeling studies (Bayer et al., 2017).

113  
114 Past studies using DGVMs mainly focused different estimates of  $E_{LUC}$  between accounting for gross land  
115 use change and net transitions only. Very few studies have addressed the issue of how much  $E_{LUC}$  from  
116 gross transitions differ by assuming clearing of primary forests versus secondary forests. The former issue  
117 can be tackled by DGVMs without sub-grid secondary lands, while the latter one can only be addressed  
118 by DGVMs with an explicit sub-grid secondary land age structure. Furthermore, it is unclear either how  
119 large the impact of shifting cultivation rotation length on the estimated  $E_{LUC}$  is.

120  
121 In this study, we quantify global and regional carbon emissions from historical gross land use change  
122 since 1501 using a global vegetation model ORCHIDEE (ORGanizing Carbon and Hydrology In Dynamic  
123 EcosystEms). The ORCHIDEE model has recently incorporated gross land use change and wood harvest,  
124 along with the representation of sub-grid secondary land cohorts. The model development and  
125 examination of model behaviour on site and regional scales are documented in a companion paper (Yue et  
126 al., 2017). The current paper focuses on the model global application. Our objectives are: 1) to quantify  
127 global and regional carbon emissions from historical gross land use change since 1501, and to examine  
128 the differences in  $E_{LUC}$  when considering sub-grid secondary land cohorts by using parallel model  
129 simulations; 2) to examine contributions to  $E_{LUC}$  from different LUC processes (i.e., net transitions only,  
130 shifting cultivation or land turnover, and wood harvest) and how they differ between the two model  
131 configurations with and without secondary land cohorts; 3) to examine the impacts of different rotation  
132 lengths in shifting cultivation on  $E_{LUC}$ . Hereafter, we will use the terms ‘shifting cultivation’ or ‘land  
133 turnover’ interchangeably as they refer to the same process in the model — bi-directional equal-area land  
134 transitions between two land use types.

135

## 136 2 Methods

### 137 2.1 ORCHIDEE-MICT model v8.4.2 and the implemented gross LUC processes

138 ORCHIDEE (Krinner et al., 2005) is a dynamic global vegetation model and the land surface component  
139 of the IPSL Earth System Model (ESM). It comprises three sub-models that operate on different time  
140 steps. The SECHIBA sub-model operates on half-hourly time steps and simulates fast exchanges of  
141 energy, water and momentum between vegetation and the atmosphere. The STOMATE sub-model  
142 operates on daily time steps and simulates vegetation carbon cycle processes including photosynthate  
143 allocation, plant phenology, vegetation mortality and recruitment. The third sub-model contains various  
144 modules of different processes on varying time steps, such as vegetation dynamics, fire disturbance and  
145 land use change.

146

147 The LUC module in ORCHIDEE was originally developed in Piao et al. (2009a), where only net  
148 transitions were taken into account. Recently, a gross land use change module, together with explicit  
149 representation of differently aged sub-grid land cohorts, have been implemented in a branch of  
150 ORCHIDEE model known as ORCHIDEE-MICT (Yue et al., 2017). This model will be henceforth  
151 referred to as ORCHIDEE-MICT v8.4.2. Idealized site-scale simulations with this model have shown that  
152 estimated carbon emissions from shifting cultivation and wood harvest are reduced by explicitly including  
153 sub-grid age dynamics, in comparison with an alternative approach to representing land cover types with  
154 a single ageless patch. This is because the secondary forests that are cleared in shifting cultivation or  
155 wood harvest with a rotation length of 15 years have a lower biomass than the mature forests that are  
156 otherwise cleared. Yue et al. (2017) provides details on the underlying processes in explaining differences  
157 in  $E_{LUC}$  regarding whether sub-grid forest age structure is considered or not.

158

159 The gross LUC module operates on an annual time step. For the very first year of the simulation, an initial  
160 land cover map (represented as a map of plant function types or PFTs) is prescribed. Land cover maps of  
161 subsequent years are updated using land use transition matrices corresponding to different LUC  
162 processes. Land use transitions between four vegetated land cover types are included: forest, natural  
163 grassland, pasture and cropland. The model separates overall LUC into three additive sub-processes in  
164 order to diagnose their individual contributions to  $E_{LUC}$ , namely net land use change equivalent to the  
165 original approach that considers net transitions only, land turnover equivalent to shifting cultivation, and  
166 wood harvest. Matrices for net land use change and land turnover ( $[X_{i,j}]$ ) take the form of 4 rows by 4  
167 columns, with  $X_{i,j}$  indicating the land transition from vegetation type  $i$  to  $j$ . The matrix for wood harvest  
168 has only two elements, indicating forest area as grid cell fractions that are subject to harvest from primary

169 and secondary forests, respectively. The current model version assumes that bare land fraction remains  
170 constant throughout the entire simulation.

171  
172 Differentiation of age classes applies on all vegetation types in the model. The number of age classes for  
173 each PFT can be customized via a configuration file. Age classes for forest PFTs are distinguished in  
174 terms of woody biomass, while those for herbaceous PFTs are defined using soil carbon stock. Newly  
175 established lands after LUC are assigned to the youngest age class. Forest cohorts move to the next age  
176 class when their woody biomass exceeds the threshold. For herbaceous PFTs, younger age classes are  
177 parameterized to have a larger soil carbon stock. This serves mainly as a preliminary attempt to have  
178 cohorts of secondary lands for herbaceous vegetation. Because the change in soil carbon depends on the  
179 vegetation types before and after LUC and on climate conditions (Don et al., 2011; Poeplau et al., 2011),  
180 ideally agricultural cohorts from different origins should be differentiated, with a origin-specific soil  
181 carbon boundary parameterization. However, to avoid inflating the total number of cohorts and the  
182 associated computation demand, as a first attempt here, we simply divided each herbaceous PFT into two  
183 broad sub-grid cohorts according to their soil carbon stocks and without considering their individual  
184 origins. We expect that such a parameterization can accommodate some typical LUC processes, such as  
185 the conversion of forest to cropland where soil carbon usually decreases over time, but not all LUC types  
186 (for instance, soil carbon stock increases when a forest is converted to a pasture).

187  
188 To simulate LUC with sub-grid land cohorts, a set of priority rules become necessary regarding which  
189 land cohorts to target given a specific LUC type (Table 1 in Yue et al., 2017), and regarding how to  
190 allocate LUC area into different PFTs of the same age class. For net LUC, clearing of forests exclusively  
191 starts from the oldest cohort and then moves onto younger ones until the youngest one. For shifting  
192 cultivation or land turnover, forest clearing starts from a pre-defined middle-aged class, and then moves  
193 onto older ones if this starting age class is used up, until the oldest ones. The primary target forest cohort  
194 in shifting cultivation and secondary forest harvest can be parameterized in the model. For the current  
195 study, shifting cultivation primarily targets the 3<sup>rd</sup> youngest cohort (Cohort<sub>3</sub>) and secondary forest harvest  
196 primarily targets the 2<sup>nd</sup> youngest cohort (Cohort<sub>2</sub>), with a total number of 6 forest cohorts (Cohort<sub>1</sub> to  
197 Cohort<sub>6</sub>, with Cohort<sub>1</sub> being the youngest) being simulated. This is to accommodate the assumption used  
198 in the LUC forcing data that shifting cultivation has a certain rotation length (see the Sect. 2.2), so that  
199 secondary forests are given a high priority to be cleared for agricultural land, and older forests will be  
200 cleared when even more agricultural lands are needed. Finally, for all other land cover types that are used  
201 as a source for conversion, as well as for primary forest harvest, we start from the oldest age class and  
202 move sequentially to younger ones in order to meet the prescribed LUC area in the forcing data. After the

203 LUC area is allocated on the cohort level, it is then distributed among different PFTs in proportion to their  
204 existing areas in this cohort.

205

206 In order to compare the simulated  $E_{LUC}$  with and without sub-grid secondary land cohorts, ORCHIDEE-  
207 MICT v8.4.2 can be run in a way that each PFT has one single age class. This is equivalent to the  
208 alternative approach by which no sub-grid land cohorts are simulated. For more information on the  
209 rationale and details of LUC implementation in ORCHIDEE-MICT v8.4.2, readers are referred to Yue et  
210 al. (2017).

211

## 212 **2.2 Preparation of forcing land use change matrices**

213 For historical land use transitions, the land use harmonized data set version 1 (LUH1) for the CMIP5  
214 project was used (Hurtt et al., 2011, [http://luh.umd.edu/data.shtml#LUH1\\_Data](http://luh.umd.edu/data.shtml#LUH1_Data)). We used the version of  
215 LUH1 data without urban lands as ORCHIDEE-MICT v8.4.2 does not simulate the effects of urban lands.  
216 The original data set is at a  $0.5^\circ$  spatial resolution with an annual time step covering 1500-2005. Four land  
217 use types are included: primary natural land, secondary natural land, pasture and cropland. The type of  
218 “natural land” consists of grassland and forest (which are separated in ORCHIDEE-MICT) but their  
219 relative fractions are not separated. In LUH1, land use transitions from either primary or secondary  
220 natural land to pasture or cropland are provided, and vice versa. Secondary natural lands originated from  
221 pasture or cropland abandonment. Besides, land use transitions between pasture and cropland are  
222 provided as well. Harvested wood comes either from primary or secondary forest or non-forest lands,  
223 with ground area fractions that are harvested being available. Note that this does not contradict with the  
224 fact that forest and grassland fractions are not separated within the land use type of “natural land”,  
225 because forests are defined as natural lands with a certain biomass carbon stock based on the simulated  
226 biomass in a terrestrial model (Hurtt et al., 2011).

227

228 Rather than the simple terrestrial model (Miami-LU) used in Hurtt et al. (2011) to separate natural  
229 vegetation into forested and non-forest land, ORCHIDEE-MICT distinguishes 8 forest PFTs, 2 natural  
230 grassland PFTs, 2 cropland PFTs (Krinner et al., 2005) and 2 pasture PFTs. Thus, to use LUH1  
231 reconstructions as a forcing input, assumptions have to be made to disaggregate LUH1 land use types into  
232 corresponding ORCHIDEE PFTs. For this purpose, we used an ORCHIDEE-compatible PFT map  
233 generated from the European Space Agency (ESA) Climate Change Initiative (CCI) land cover map  
234 (shortened as the ESA-CCI-LC map) covering a 5-year period of 2003-2007 (European Space Agency,  
235 2014), assuming that it corresponds to the land use distribution for 2005 by the LUH1 data. Subsequently,  
236 we backcast historical PFT map time series for 1500-2004 based on this 2005 PFT map using LUH1

237 historical net land use transitions as a constraint. Because land turnover involves an equal, bi-directional  
238 land transition between two land cover types, it does not lead to any net annual changes in the PFT map.  
239 Therefore, only net transition information is needed when backcasting historical PFT maps.

240

241 To separate land use transitions in LUH1 into processes of net land use change and land turnover, we  
242 simply treat net land use change as the land transitions excluding the minimum reverse fluxes between  
243 two land use types. During the backcasting process, reconciliations have to be made where LUH1 data  
244 disagrees with the ESA map on the grid cell scale. When backcasting historical PFT map time series  
245 using net land use change matrices, we assume that when pasture or cropland is created, they come from  
246 an equal share of forest and grassland; when their fractions decrease, cropland abandonment leads first to  
247 forest recovery and then followed by natural grassland expansion, while pasture abandonment leads to an  
248 equal share of forest and natural grassland expansion. We then treat the minimum of two reverse land  
249 fluxes between secondary natural land and cropland or pasture as land turnover transitions. For each year,  
250 the land turnover transition between two land use types is not allowed to exceed the minimum of their  
251 existing areas. Spatially resolved forest harvest time series are provided in LUH1. We built the wood  
252 harvest matrices by limiting wood harvest area within the total area of forest PFTs over each grid cell for  
253 each year. Primary and secondary forest wood harvests from LUH1 were included and treated as primary  
254 and secondary forest harvest in the model, respectively, with non-forest wood harvest being discarded.  
255 More details on PFT map backcasting and the construction of land use transition matrices are provided in  
256 the Supplement Material.

257

258 The construction of historical PFT maps and land transition matrices was done at 2° resolution for the  
259 whole globe, after re-sampling all input data from their original resolution to 2°. The reconstructed global  
260 forest area agrees with that by Peng et al. (2017), who has backcast historical ORCHIDEE PFT map  
261 series using the same ESA-CCI-LC 2005 PFT map and historical pasture and crop distributions from  
262 LUH1 but not the LUH1 land use transitions, with historical forest areas in the nine regions of the globe  
263 being constrained by data in Houghton (2003) based on national forest area statistics. The land turnover  
264 transitions between secondary land (forest and grassland) and cropland (or pasture) from the matrices  
265 defined above are smaller than originally prescribed in LUH1, because some of the prescribed transitions  
266 are ignored due to the inconsistency between LUH1 map in 2005 and the 2005 ORCHIDEE PFT map  
267 (See Supplement Material for detailed comparison). Because of this inconsistency, around 35% of net  
268 transitions from natural land to pasture, and 14% of net transitions from natural land to cropland were  
269 omitted when adapting the LUH1 data set to our model. About 20% of the turnover transitions between  
270 secondary land and pasture were omitted, and 11% of turnover transitions between secondary land and



271 cropland were omitted. Such inconsistencies among different data sets are a rather common challenge for  
272 their application in DGVMs, which have been reported by, for example, in Li et al. (2017), Meiyappan  
273 and Jain (2012) and Peng et al. (2017). Note that shifting cultivation (land turnover) is limited to the  
274 tropical band as in LUH1, and the land turnover change resulting from the gridded LUH1 data upscaling  
275 from 0.5° to 2° is not included. The missing land turnover areas represent 17% of the turnover between  
276 natural lands and cropland that are included in our study, and 14% of the turnovers between natural lands  
277 and pasture.

278

## 279 **2.3 Simulation protocol**

### 280 **2.3.1 Separate contributions of different land use change processes**

281 The PFT map of year 1500 as generated from the backcasting procedure (see the previous section) was  
282 used during the model spin-up. Climate data used were CRUNCEP v5.3.2 climate forcing at 2° resolution  
283 covering 1901-2013 (<https://vesg.ipsl.upmc.fr/thredds/fileServer/store/p529viov/cruncep/readme.html>).  
284 For the spin-up, climate data were cycled from 1901 to 1910, with atmospheric CO<sub>2</sub> concentration being  
285 fixed at the 1750 level (277 ppm). Following LUH1 (Hurtt et al., 2011), we assume that no land use  
286 change occurs during the model spin-up. This might lead to overestimation of E<sub>LUC</sub> for the beginning  
287 years of the transient simulation due to high carbon stocks that are free from LUC before 1501. But on the  
288 other hand, legacy emissions from LUC activities before 1501 are also omitted. In general, because the  
289 magnitude of annual LUC activities for 1501–1520 is very small (Fig. 2), we assume that the bias in E<sub>LUC</sub>  
290 induced by not including LUC in the spin-up is small. Besides, simulated E<sub>LUC</sub> is less influenced by this  
291 factor after ca. 1700, which dominates the cumulative E<sub>LUC</sub> since 1501. The spin-up lasts for 450 years  
292 and includes a specific accelerated soil carbon module to speed up the equilibrium of soil carbon stock.  
293 Fires and fire carbon emissions are simulated with a prognostic fire module (Yue et al., 2014), with fire  
294 occurring only on forests and natural grasslands. Simulated net land-atmosphere carbon flux is calculated  
295 as net biome production (NBP):

296

$$297 \text{NBP} = \text{NPP} - F_{\text{Inst}} - F_{\text{Wood}} - F_{\text{HR}} - F_{\text{Fire}} - F_{\text{AH}} - F_{\text{pasture}} \quad \text{Eq (1)}$$

298

299 Where NPP is the net primary production. All fluxes starting with “F” are outward fluxes (i.e., carbon  
300 fluxes from ecosystems to the atmosphere), with F<sub>Inst</sub> being instantaneous carbon fluxes lost during LUC  
301 (e.g., site preparation, deforestation fires etc.), F<sub>Wood</sub> for delayed carbon emissions from the degradation of  
302 harvested wood product pools, F<sub>HR</sub> for soil respiration, F<sub>Fire</sub> for carbon emissions from natural and  
303 anthropogenic open vegetation fires, F<sub>AH</sub> for carbon emissions from agricultural harvest, including harvest  
304 from croplands and pastures (treated as a carbon source for the year of harvest equaling the harvested

305 biomass; this source is assumed to occur over the grid cell being harvested, ignoring the transport,  
306 processing and final consumption of agricultural yield), and  $F_{\text{pasture}}$  for additional non-harvest carbon  
307 sources from pastures including export of animal milk and methane emissions.  $E_{\text{LUC}}$  is quantified as the  
308 differences in NBP between simulations without and with LUC, with positive values representing carbon  
309 sources.

310

311 We conducted a set of additive factorial simulations (S0 to S3) by including matrices of different LUC  
312 processes in each simulation (Table 1), which allows diagnosing  $E_{\text{LUC}}$  from different LUC processes.  
313 Note that this separation is done from a theoretical point of view with the objective to investigate the  
314 impacts on  $E_{\text{LUC}}$  from gross land use change when including sub-grid multiple land cohorts. The  
315 simulations of S0 to S3 allow separating the contributions to  $E_{\text{LUC}}$  by different LUC processes in a fully  
316 additive manner and this works accurately for a linear system. To test the uncertainties in  $E_{\text{LUC turnover}}$  and  
317  $E_{\text{LUC harvest}}$  introduced by this assumption, we performed an alternative S2b simulation, which includes net  
318 land use change and wood harvest.  $E_{\text{LUC turnover}}$  and  $E_{\text{LUC harvest}}$  are then calculated using both S2 and S2b  
319 simulations and emissions from these two factorial runs are compared with each other. Henceforth for  
320 brevity, we denote the simulation without sub-grid age class dynamics as  $S_{\text{ageless}}$ , simulation with sub-  
321 grid age dynamics as  $S_{\text{age}}$ . At last, to investigate the sensitivity of  $E_{\text{LUC turnover}}$  to shifting cultivation  
322 rotation length, we performed further simulations for Africa as a case study. Another five simulations  
323 were branched from the S2 simulation starting from the year 1860, in which the primary target cohort for  
324 land turnover was varied as each of the five cohorts other than Cohort<sub>3</sub>, the default primary target cohort  
325 for land turnover.

326

### 327 2.3.2 Define thresholds for age classes

328 For the simulation with age dynamics ( $S_{\text{age}}$ ), six age classes are used for forest PFTs and two age classes  
329 for other PFTs. As explained, age classes of forest PFTs are separated in terms of woody biomass. The  
330 LUH1 data assumes a 15-year residence time for agricultural land in shifting cultivation in tropical  
331 regions. Ideally, model parameterization of woody biomass thresholds should allow corresponding forest  
332 age being inferred, so that clearing of forest age class in the model could match that in the LUH1 data set.  
333 For this purpose, we fit a woody biomass-age curve for each forest PFT using the model data from the  
334 spin-up:

335

$$336 \quad B = B_{\text{max}} \times [1 - \exp(-k \times \text{age})] \quad \text{Eq (2)}$$

337

338 where  $B_{\max}$  is the asymptotic maximum woody biomass;  $k$  is the biomass turnover rate (in unit of  $\text{yr}^{-1}$ ).  
339 The curve-fitting used PFT-specific woody biomass time series during spin-up by averaging all grid cells  
340 across the globe. The ratios of woody biomass thresholds for each age class to the maximum woody  
341 biomass ( $B_{\max}$ ) are looked up from this curve, based on their corresponding forest ages (Table 2). Next,  
342 these ratios are multiplied with the equilibrium woody biomass at each grid cell, approximated by the  
343 woody biomass at the end of model spin-up, to derive a spatial map of thresholds in woody biomass. We  
344 set the corresponding age for the Cohort<sub>3</sub> for tropical forests as 15 years, in line with the residence time of  
345 shifting cultivation assumed in LUH1. Considering that temperate and boreal forests grow slower than  
346 tropical ones, forest ages corresponding to the Cohort<sub>3</sub> are set as 20 and 30 years for temperate and boreal  
347 forests, respectively.

348

349 We acknowledge that using such static woody biomass boundaries cannot ensure a forest of an exact  
350 given age to be cleared in the transient simulations, because changes in environmental conditions (e.g.,  
351 atmospheric  $\text{CO}_2$  concentrations, climate) may alter the woody biomass-age curves established from the  
352 spin-up results. For example, the boundary biomass limits may be reached at an earlier age in case  
353 productivity increases due to changes in environmental conditions. If we assume that land managers  
354 always clear forest according to their ages, then our simulated  $E_{\text{LUC}}$  might be underestimated, provided a  
355 higher biomass for a given age in transient simulations than that in the spin-up. But the uncertainties  
356 resulting from using static biomass boundaries should be less influential than the uncertainty induced by  
357 the fact that in general, rotational lengths of land turnover are poorly known and that a constant 15-year  
358 length for shifting agriculture in tropical regions is assumed (Hurtt et al., 2011). For wood harvest, we  
359 also assumed three different fixed rotation lengths for boreal, temperate and tropical regions, respectively  
360 (Table 2).

361

362 We used two age classes for each herbaceous PFT including natural grassland, cropland and pasture,  
363 representing high versus low soil carbon densities, respectively. The energy balance in ORCHIDEE-  
364 MICT v8.4.2 is resolved over the whole grid cell, and the hydrological balance is calculated over sub-grid  
365 soil tiles (bare soil, forest and herbs) rather than over each PFT. We thus expect the factors influencing  
366 soil carbon decomposition (i.e., soil temperature, soil moisture) to have little difference between different  
367 age classes of the same PFTs. This justifies the small number of age classes for herbaceous PFTs selected  
368 here as it can maximize computing efficiency. Overall, this feature of separating herbaceous PFTs into  
369 multiple cohorts is coded more as a “place holder” for the current stage of model development. Fully  
370 tracking soil carbon stocks of different vegetation types and their transient changes following LUC would  
371 require a much larger number of cohorts than that used in this study.

372

373 In  $S_{age}$  simulations, clearing of forest in the process of land turnover starts from Cohort<sub>3</sub>, corresponding to  
374 15 year-old forest, and forest clearing for wood harvest starts from Cohort<sub>2</sub>. Wood product pools resulting  
375 from net LUC and land turnover, and those from wood harvest are tracked separately in the model.

376 However, land patches created from different LUC activities are not tracked individually, e.g., young  
377 forests, either re-established from land turnover or wood harvest, are merged together. In this approach, it  
378 is not possible to attribute the carbon fluxes into exact individual LUC processes, which explains why  
379 factorial simulations are needed. Within the model, wood harvest module is executed before the modules  
380 of net land use change and land turnover. This is reasonable as a forest might be harvested prior to being  
381 converted to agricultural land. Last, we turned off the dynamic vegetation module because allowing  
382 dynamic vegetation and using prescribed backcast historical land cover maps are internally inconsistent.

383

### 384 **3 Results**

#### 385 **3.1 Global carbon emissions with and without sub-grid age dynamics**

386 Cumulative  $E_{LUC}$  during 1501–2005 for different LUC processes and model configurations are shown in  
387 Table 3. The model simulates a cumulative  $E_{LUC\ net}$  of 123.7 and 118.0 Pg C during 1501–2005, for cases  
388 of without and with sub-grid age dynamics, respectively. Including land turnover and wood harvest yields  
389 additional carbon emissions, with the cumulative  $E_{LUC\ turnover}$  as 45.4 Pg C and  $E_{LUC\ harvest}$  as 27.4 Pg C in  
390  $S_{ageless}$  simulations. Accounting for age dynamics, in contrast, generates an  $E_{LUC\ turnover}$  of 27.3 Pg C, 40%  
391 lower than that obtained by the  $S_{ageless}$  simulation. The cumulative  $E_{LUC\ harvest}$  for  $S_{age}$  equals to 30.8 Pg C  
392 and is slightly higher than in  $S_{ageless}$ . When wood harvest is included on top of only the net land use  
393 change (the S2b simulation), the  $E_{LUC\ harvest\ S2b}$  obtained by differing S1 and S2b simulations is slightly  
394 higher than that when wood harvest is included as the last term (i.e., quantified by differing S2 and S3  
395 simulations). This is reasonable because in the latter case, forests subject to wood harvest were already  
396 under disturbances of both land turnover and net land use change, which reduce forest biomass carbon  
397 stocks for harvest. The  $E_{LUC\ turnover}$  derived from S2b simulations, in contrast, is lower than that derived  
398 from S2 simulations (Table 3). Nonetheless, a consistent lower  $E_{LUC\ turnover}$  is obtained by accounting for  
399 sub-grid age dynamics than not, by 40% or 37% depending whether the S2 or S2b simulations are used.  
400 Furthermore, different estimations of  $E_{LUC\ turnover}$  derived by S2 and S2b simulations are close to each  
401 other, with a difference of ~10% of their mean value, indicating that LUC emissions are a quasi-linear  
402 system with respect to the different LUC processes. Based on this and for simplicity, in the following we  
403 will mainly focus on the results using S2 simulations.

404

405 Figure 1 shows the time series of simulated  $E_{LUC, all}$  from all LUC processes (net land use change + land  
406 turnover + wood harvest) in comparison with previous studies. Simulated  $E_{LUC}$  from each individual LUC  
407 process and corresponding time series of LUC areas are shown in Fig. 2. The temporal changes in  
408 emissions from S2b simulations are shown in Fig. S7. All estimations show a gradual increase of  $E_{LUC}$   
409 starting from the early 18<sup>th</sup> century with a peak of 1.5–3.5 Pg C yr<sup>-1</sup> around the 1950s, followed by a  
410 slight decrease during 1970s and 1980s and then another peak appeared during 1990s.  $E_{LUC}$  simulated by  
411 ORCHIDEE-MICT v8.4.2 is at the lower bound of all estimations until 1950s, but its second peak of  
412 emissions around 1990s (1.7–1.8 PgC yr<sup>-1</sup>) is a little higher than the first one (1.5 Pg C yr<sup>-1</sup>).  $E_{LUC, all, ageless}$   
413 remains slightly higher than  $E_{LUC, all, age}$  until ca. 1960, and after that the difference increases to 0.25 Pg C  
414 yr<sup>-1</sup>. This two-peak pattern over time in  $E_{LUC, all}$  by ORCHIDEE-MICT v8.4.2 is mainly driven by  $E_{LUC, net}$   
415 (Fig. 2a) which also shows two peaks around 1950s and 1990s, consistent with the peaks of land use  
416 change areas in the LUH1 forcing data (Fig. 2d). It should also be noted that as  $E_{LUC}$  is quantified as the  
417 difference in NBP between two model simulations, its magnitude thus depend both on the areas subject to  
418 LUC and the magnitude of carbon fluxes in the reference S0 simulations, as driven by climate variability,  
419 atmospheric CO<sub>2</sub>, etc.

420

421 Consistent with the idealized site-scale simulation in Yue et al. (2017),  $E_{LUC, turnover, ageless}$  is higher than  
422  $E_{LUC, turnover, age}$  (Fig. 2b). Emissions from instantaneous fluxes and harvested wood product pool are lower  
423 in the  $S_{age}$  than in  $S_{ageless}$  because in the former case low-biomass secondary forests are converted to  
424 agricultural land, as opposed to high-biomass mature forests in the latter one. Similarly, the lower  $E_{LUC}$   
425  $_{turnover}$  in the  $S_{age}$  simulation than  $S_{ageless}$  are also found in the results with the S2b simulation (Fig. S7). The  
426 difference in  $E_{LUC, turnover}$  explains most of the difference in  $E_{LUC, all}$  between  $S_{age}$  and  $S_{ageless}$ , since  $E_{LUC, net}$   
427 does not differ much (Fig. 2a). The similar estimates of  $E_{LUC, net}$  are because the cleared forests in net LUC  
428 have little difference in their biomass densities between  $S_{ageless}$  and  $S_{age}$ . Both  $E_{LUC, turnover, ageless}$  and  $E_{LUC}$   
429  $_{turnover, age}$  roughly follow the temporal pattern of areas impacted by land turnover from LUH1 (Fig. 2e),  
430 with a steep increase starting from ca. 1900 until 1980, corresponding to a strong increase in the areas  
431 undergoing forest-pasture land turnover. After 1980 the turnover-impacted area stabilizes and then shows  
432 a slight decrease. Accordingly,  $E_{LUC, turnover, ageless}$  shows a slight decrease of emissions in Fig. 2b, while  
433  $E_{LUC, turnover, age}$  has a much stronger decrease, driven by the fact that recovering secondary forests gain  
434 carbon quickly after being taken out of shifting agriculture systems.

435

436 Finally,  $E_{LUC, harvest}$  between  $S_{age}$  and  $S_{ageless}$  simulations are almost identical until 1800 (Fig. 2), during  
437 which the wood harvest area remains stable (Fig. 2f). After this,  $E_{LUC, harvest, ageless}$  is lower than  $E_{LUC, harvest,}$   
438  $_{age}$  for the 19<sup>th</sup> and most of the 20<sup>th</sup> century when  $E_{LUC, harvest}$  continued to rise, mainly driven by a rise in

439 secondary forest harvest area (Fig. 2f). According to the priority rules of secondary forest harvest in  $S_{age}$ ,  
440 older forests, until the oldest ones, will be harvested if existing young forests cannot meet the prescribed  
441 harvest target. This most likely happens when harvested area continues to rise. This exemplifies the  
442 potential inconsistencies between model structure and forcing data. In addition, under such a  
443 circumstance, old forests in  $S_{age}$  simulation tend to have higher biomass density than the ageless forests in  
444  $S_{ageless}$ , because in  $S_{age}$  these mature forests remain intact throughout the whole simulation, while in  $S_{ageless}$   
445 they are “degraded” due to all kinds of historical LUC activities. This explains the slightly higher  $E_{LUC}$   
446  $_{harvest}$  in the  $S_{age}$  simulation. Similarly, it also explains that the difference in  $E_{LUC}$   $_{harvest}$  between  $S_{ageless}$  and  
447  $S_{age}$  from S2b simulations is smaller than that from S2. In S2b simulations,  $E_{LUC}$   $_{harvest}$  is quantified by  
448 including harvest on top of net LUC only, and the harvested forests have not been affected by land  
449 turnover, so  $E_{LUC}$   $_{harvest}$  in the end differs little between  $S_{ageless}$  and  $S_{age}$ .

450

### 451 **3.2 Spatial distribution of land use change emissions**

452 Figure 3 shows the spatial distribution of cumulative  $E_{LUC}$  for 1501–2005 from different LUC processes  
453 in  $S_{ageless}$  (Fig. 3a, 3d, 3g), the difference in  $E_{LUC}$  between  $S_{age}$  and  $S_{ageless}$  (Fig. 3b, 3e, 3h), corresponding  
454 net forest area change (Fig. 3c) and areas subject to land turnover (Fig. 3f) and wood harvest (Fig. 3i).  
455 The spatial pattern of  $E_{LUC}$   $_{net}$  generally resembles that of forest area loss, with large areas of forests being  
456 cleared and corresponding high  $E_{LUC}$   $_{net}$  in eastern North America, South America and Africa, southern  
457 and eastern Asia, and in central Eurasia (Fig. 3a, Fig. 3c). Central and Eastern Europe show some  
458 increases in forest area but carbon emissions from net land use change persists, probably because forest  
459 recovery happened recently and carbon accumulation in recovering forests is not yet large enough to  
460 compensate for historical loss (e.g., see Fig. 5g). Depending on different regions,  $E_{LUC}$   $_{net, age}$  is slightly  
461 higher (e.g., along the boreal forest belt in central Europe and Asia, woodland savanna in South America)  
462 or lower (e.g., part of Africa and Australia) than  $E_{LUC}$   $_{net, ageless}$  (Fig. 3b). This difference between  $S_{age}$  and  
463  $S_{ageless}$  is generally small ( $<0.5$  kg C m<sup>-2</sup> over 1501-2005). It mainly depends on the age classes of forests  
464 to be cleared in  $S_{age}$  and how the forest biomass density compares with that from  $S_{ageless}$  and whether  
465 biomass density of the single ageless mature patch is reduced or not with establishment of young forests.  
466

467 Shifting cultivation is limited to the tropical region (Fig. 3h), as in the original LUH1 forcing data.  
468 Tropical Africa is the region with most of the land turnover activities, and consequently has highest  $E_{LUC}$   
469  $_{turnover}$ . Note that the peripheral of Amazon basin also shows active shifting cultivations and resulting  
470 carbon emissions (Fig. 3b, Fig. 3f).  $E_{LUC}$   $_{turnover, age}$  is in general lower than  $E_{LUC}$   $_{turnover, ageless}$  everywhere  
471 except at the northern fringe of African woodland savanna (Fig. 3e). Last, wood harvest mainly occurs in  
472 temperate and boreal forest in Northern Hemisphere (Europe and central Siberia, eastern North America

473 and southern and eastern Asia) and tropical forests including those of Amazon forest, in central Africa  
474 and tropical Asia, with corresponding carbon emissions (Fig. 3c, Fig. 3i).  $E_{LUC\ harvest, age}$  is a higher source  
475 than  $E_{LUC\ harvest, ageless}$  for most of the harvested regions, which mainly results from the model feature as  
476 explained above.

477

### 478 **3.3 Simulated regional LUC emissions**

479 Estimated carbon emissions since 1900 from different regions are shown in Fig. 4, with emissions from  
480 each LUC source for  $S_{ageless}$  being shown in Fig. S8. The corresponding areas subject to the three LUC  
481 processes with forests being mainly involved are shown in Fig. 5. As shown in Fig. 5, in spite of incessant  
482 episodic forest gains, for most time in most regions, historical net forest change was dominated by forest  
483 loss, except for the second half of the 20<sup>th</sup> century in Western Europe, Former Soviet Union (FSU), and  
484 for the time period after 1970 in Pacific Developed Region. Meanwhile, land turnover and wood harvest  
485 persisted in most regions, although their magnitudes varied over time. While forest gain can lead to  
486 carbon uptake, it could be outweighed by emissions from simultaneous forest loss (note here both forest  
487 loss and gain occurred as a result of net LUC within the same region but not within the same grid cell),  
488 land turnover and wood harvest. Thus it is not surprising that LUC impacts on carbon cycle are diagnosed  
489 as emissions in most regions for most time, except for the latter half the 20<sup>th</sup> century for Former Soviet  
490 Union (Fig. 4).

491

492 We also compared our estimates with those from Stocker et al. (2014). Stocker et al. (2014) simulated  
493 LUC emissions using a different vegetation model (LPX-Bern) but attributed the contributions of each  
494 individual LUC process using a similar approach as ours. Both studies are forced by the LUH1 data set,  
495 although actual areas undergoing different LUC activities may slightly differ because of different LUC  
496 implementation strategies. The two estimates of LUC emissions from our study and Stocker et al. (2014)  
497 are in general agreement for most of the regions, including their temporal variations (Fig. 4). Global  
498 emissions are dominated by Central and South America and Africa & Middle East. Emissions increased  
499 in both regions since 1900, and a peak of emissions occurred around the middle of the 20<sup>th</sup> century in  
500 Africa and around 1980 in Central and South America (Fig. 4a, 5b). Emissions from Stocker et al. (2014)  
501 show similar temporal variations in these two regions. The peak of emissions in Africa & Middle East  
502 around 1950 is caused by a peak of forest loss due to net LUC (red line in Fig. 5b), and a surge of forest  
503 loss due to land turnover that has accelerated between 1940 and 1960 (green line in Fig. 5b). After that  
504 emission peak, emissions slightly decreased, mainly due to the stabilized land turnover activities and a  
505 drop in area of net LUC. Then the emissions slightly increased again around 1980s, due to an increase in  
506 forest loss of net LUC (red line in Fig. 5b) and wood harvest (cyan line in Fig. 5b). In contrast, even with

507 a similar peak of forest loss due to net LUC in Central and South America as in Africa & Middle East  
508 around 1950s (red line in Fig. 5a), emissions in the former region continued to increase until 1980s (Fig.  
509 4a), mainly due to the continuous forest losses resulting from expanding land turnover areas (green line in  
510 Fig. 5a).

511  
512 Both South & Southeast Asia and China Region showed steady increase in emissions up to c.a. 1990s  
513 (Fig. 4c, 4d). In the former region, it is likely driven by continuously growing land turnover and wood  
514 harvest; in the latter region, it is more driven by growing net forest loss (Fig. 5c, 5d). The peak in  
515 emissions around 1990s in China Region echoes a peak in net forest loss (red line in Fig. 5d). Stocker et  
516 al. (2014) shows slightly higher emissions than our estimates for South & Southeast Asia, and lower  
517 magnitude in China Region, but with similar temporal patterns in both regions. For the three regions  
518 where land turnover activities are included in the LUH1 data set (i.e., Central and South America, Africa  
519 & Middle East and South & Southeast Asia), there are some periods during which  $E_{LUC\ ageless}$  is clearly  
520 higher than  $E_{LUC\ age}$ . They mainly correspond to the time when land turnover area either showed  
521 decelerated growth or stabilized, being roughly after 1970 in Central and South America (Fig. 4a), 1965-  
522 1985 in Africa & Middle East (Fig. 4b), and after 1980 in South & Southeast Asia (Fig. 4c).

523  
524 North America shows most clearly the legacy impact of past LUC activities on LUC emissions. For the  
525 period 1900–1940, carbon emissions in North America gradually decreased even though areas subject to  
526 forest loss and wood harvest showed slight increases (Fig. 4e, Fig. 5e). This is likely due to the fact that a  
527 peak of net forest loss occurred preceding 1900, which yields a high emission legacy for the beginning  
528 years of the 20<sup>th</sup> century (data not shown). LUC emissions and sinks in Pacific Developed Region and  
529 Europe are very small, despite a high forest wood harvest area in Europe. This is because in general  $E_{LUC}$   
530  $_{harvest}$  is small compared to  $E_{LUC\ net}$ , probably due to the biomass accumulation in re-growing forest after  
531 wood harvest (Fig. S8). The carbon sink as a result of net forest gain is the most prominent in Former  
532 Soviet Union (blue line in Fig. 5h), where a peak of forest gain around 1950s lead to a sustained sink of  
533  $\sim 0.1\text{ PgC yr}^{-1}$  for the second half of the 20<sup>th</sup> century (Fig. 4h). However, concurrent sink is not seen in  
534 Stocker et al. (2014) (Fig. 4h).

535

## 536 **4 Discussion**

### 537 **4.1 Impacts on estimated $E_{LUC}$ by including gross LUC and sub-grid secondary forests**

538 The advancement in this study in comparison with previous works, as far as we know, is the explicit  
539 inclusion of differently aged sub-grid secondary land cohorts in a DGVM. Although secondary lands have  
540 been represented in some DGVMs in previous studies (Shevliakova et al., 2009; Stocker et al., 2014;



541 Yang et al., 2010), here we incorporated the concept of rotation cycle. This is particularly important in  
542 simulating the carbon cycle impacts of gross LUC, such as wood harvest and shifting cultivation that  
543 often have certain rotation cycles. Because secondary lands, especially young re-growing forests, have  
544 lower biomass carbon stock than primary mature forests, the simulated  $E_{LUC}$  involving secondary lands  
545 tend to be lower than that from simulations without sub-grid age dynamics. Our results demonstrate that  
546 by explicitly including secondary forest cohorts, cumulative  $E_{LUC}$  from shifting cultivation in tropical  
547 regions during 1501–2005 are reduced from 45.4 Pg C to 27.4 Pg C, or 40% lower. Nonetheless, it should  
548 be noted that these results are based on a constant 15-year rotation length in shifting cultivation, to be  
549 consistent with the LUH1 data. To test the sensitivity of  $E_{LUC\ turnover}$  to different rotation lengths in  $S_{age}$   
550 simulations, we performed additionally five alternative S2 simulations, all starting from 1861 based on  
551 the system state of 1860 obtained by the default S2 simulation, but with the primary target cohort in land  
552 turnover varying among the other five cohorts except Cohort<sub>3</sub> (the default target cohort). The results are  
553 presented in Fig. S9.  $E_{LUC\ turnover}$  over 1861–2005 increases in a roughly linear way with the assumed  
554 woody mass of forest cohorts that are cleared in shifting cultivation, with an increase of 5.3 Pg C in  
555 emissions per kg C m<sup>-2</sup> increase in cohort woody mass.  $E_{LUC\ turnover, ageless}$  is slightly higher than  $E_{LUC\ turnover, age}$   
556 when cohorts with ~15 years are cleared primarily. Increasing rotation lengths thus leads to higher  
557 emissions than in  $S_{ageless}$  simulations in this case. This highlights the importance of the rotation length, i.e.  
558 the residence time of agriculture in shifting cultivation systems, for the estimates of  $E_{LUC\ turnover}$ .

559  
560 Table 4 summarized estimates of  $E_{LUC}$  from different studies by including both net transitions and gross  
561 land use change, and the contributions to total emissions by including gross LUC. All studies show that  
562 including gross LUC increased estimated carbon emissions. Stocker et al. (2014) reported that gross LUC  
563 contributed 15% to total emissions, whereas Wilkenskjeld et al. (2014) reported a much higher  
564 contribution of 38%. Using a bookkeeping model, Hansis et al. (2015) reported a 22–24% contribution  
565 from gross change if primary lands are cleared, in contrast to a small contribution of only 2% if secondary  
566 lands are cleared. For  $S_{ageless}$  in the current study, the contribution of gross LUC to the total emissions is  
567 20%, falling in between Stocker et al. (2014) and others including the 28% contribution by gross LUC in  
568 the tropics reported by Houghton (2010). However, the simulation by including secondary land (i.e.,  $S_{age}$ )  
569 gives a lower gross LUC contribution (15%) than  $S_{ageless}$ . In general, the same model yields lower  
570 contribution of gross changes by converting dominantly secondary land than primary land (our study and  
571 Hansis et al., 2015). Among different models/methods, the ones including secondary lands (Houghton,  
572 2010; Stocker et al., 2014) tends to yield lower contribution of gross changes than those do not  
573 (Wilkenskjeld et al., 2014). Although the percentage might differ depending on the amount of gross LUC

574 included and the biomass stocks of the secondary lands being cleared, it seems that contributions from  
575 gross LUC are lower when including sub-grid secondary lands.

576  
577 We also expected  $E_{LUC}$  from wood harvest to be smaller when including secondary forests, for the same  
578 reason than shifting cultivation. However, we obtained a slightly higher  $E_{LUC\ harvest, age}$  than  $E_{LUC\ harvest, ageless}$ ,  
579 mainly because there are not enough secondary forests available for harvesting in  $S_{age}$ , so that mature  
580 forests with a higher biomass density than in  $S_{ageless}$  are harvested according to the priority setting in the  
581 model, which leads to higher emissions. This model feature was designed to solve the potential  
582 inconsistencies between prescribed harvest area in the forcing data and (secondary) forest availability in  
583 the model, to ensure that ultimately realized harvest area in the model is as close as possible to the  
584 prescribed one. From the S2b simulations where wood harvest, instead of land turnover, is added on top  
585 of net land use change,  $E_{LUC\ harvest}$  derived from  $S_{age}$  and  $S_{ageless}$  are very similar because in both  
586 simulations, forests with biomass close to the one of primary forests are harvested. Finally, it should be  
587 noted that reconstructions of forest wood harvest are highly uncertain. For example, LUH1 data provides  
588 a total wood harvest amount of 102 Pg C for 1850–2005 over forest and non-forest areas, whereas  
589 Houghton and Nassikas (2017) estimated 130 Pg C. Our estimates of  $E_{LUC\ harvest}$  using different  
590 approaches is 22.5–27.8 Pg for 1850–2005, close to the estimated 25.3 Pg C for 1850–2015 by Houghton  
591 and Nassikas (2017).

592  
593 In the current study, we implemented wood harvest based on input (LUC forcing) information on  
594 harvested area rather than on wood volume or biomass. In the future, this process should be modified so  
595 that harvested wood volume or biomass information is directly used in the model, to allow dynamic  
596 decision on whether an old forest or secondary forest should be harvested. Using wood harvest volume or  
597 biomass information would largely alleviate the uncertainty brought about by the unknown wood harvest  
598 rotation length because the total amount of harvested biomass would be constrained (Houghton and  
599 Nassikas, 2017).

600  
601 We do not account for any LUC activities in the spin-up run and pristine ecosystems are assumed at the  
602 beginning of the transient run in 1501. This set-up might cause a spike in emissions during the beginning  
603 years in the transient simulation because ecosystem biomass stocks are high. Such a spike was evident in  
604 results by Stocker et al. (2014, blue and green lines in their Fig. 2) when land turnover is not accounted  
605 for during the spin-up in some of their simulations. The similar model behaviour also presents in the  
606 results by Hansis et al. (2015, dark and light blue lines in their Fig. 4) using a bookkeeping model. In our  
607 study, a similar initial spike in  $E_{LUC}$  shortly after 1501 is almost invisible for the net LUC and land

608 turnover (Fig. 2a–b), probably owing to very small magnitudes of LUC area within the few years after  
609 1501 (Fig. 2d–e). However, there is a clear peak in  $E_{LUC\ turnover}$  around 1520s (Fig. 2c), a likely impact of  
610 ignoring spin-up LUC process, given that a significantly larger-than-zero harvest area is prescribed for  
611 this period (Fig. 2f). In general, the impacts of not including LUC in the spin-up process seem to be small  
612 in our results. This issue impacts much less the comparisons focusing on emissions starting from 1850 in  
613 Table 3.

614  
615 As shown in Fig. 2 and Table 3, our estimations of historical LUC emissions from both  $S_{ageless}$  and  $S_{age}$   
616 simulations are lower than other studies for most time of history (albeit close to Stocker et al. 2014 before  
617 ca. 1860). We compared in Table S1 the cumulative  $E_{LUC}$  for 1850-2005 by our studies and several  
618 previous studies. Our estimates (147 Pg C for  $E_{LUC\ age}$  and 158 Pg C for  $E_{LUC\ ageless}$ ) are lower than the  
619 lower bound of other estimates (171 Pg C by Stocker et al. 2014). Estimations of Hansis et al. (2015) and  
620 Gasser and Ciais (2013) using Hurtt et al. (2011) data set give rather larger estimates than others, being  
621 261 and 294 Pg C, respectively. The median value of all previous estimates cited in Table S1 yields 210  
622 Pg C, still much higher than our estimates.

623  
624 The lower estimates of  $E_{LUC}$  in our study are likely linked with underestimated global biomass carbon  
625 stock in ORCHIDEE-MICT V8.4.2. The global biomass carbon stock simulated by our model at 1500  
626 prior to any land use change is 365 Pg C, and increases to 510 Pg C at 2005 in the S0 simulations (i.e.,  
627 assuming no LUC activity). The simulated contemporary global biomass in the S3 simulations, where all  
628 three LUC processes are included, remains almost the same as the 1500 value. So the  $E_{LUC}$  basically  
629 balances out what would have been gained in the global biomass brought about by the environmental  
630 changes. Avitabile et al. (2016) have constructed a global contemporary aboveground biomass carbon  
631 map by merging two tropical aboveground forest biomass data sets of Saatchi et al. (2011) and Baccini et  
632 al. (2012) with northern hemisphere volumetric forest stock data from Santoro et al. (2015). Their  
633 estimated global forest biomass for aboveground only is 505 Pg C. Our simulated contemporary global  
634 total biomass stock (i.e., from S3 simulations) is thus even lower than their estimate for aboveground  
635 biomass only. Besides, some of the land transitions in LUH1 data were ignored because of the  
636 inconsistencies between LUH1 data and the model PFT map (Sect. 2.2), which may also explain the  
637 lower  $E_{LUC}$  in our estimation.

638

#### 639 **4.2 Land use and management processes in DGVMs in relation to forest demography**

640 Forest demography is an important factor in determining forest carbon dynamics on both stand and  
641 regional scales (Amiro et al., 2010; Pan et al., 2011). Natural disturbances (such as fire, wind and insect)

642 and land use change including land management are two primary factors creating spatial heterogeneity in  
643 forest age. As more and more forests are now under human management with different intensities (Erb et  
644 al., 2017; Luysaert et al., 2014), sub-grid forest demography should be incorporated in DGVMs to  
645 account for the management consequences. Furthermore, when making more accurate (and detailed)  
646 account of regional carbon balances with land use change, other land cover types than forests should be  
647 distinguished into different cohorts as well, because the presence of many nonlinear processes (e.g., soil  
648 carbon decomposition) makes the simple averaging scheme — as in the case where they are represented  
649 with a single patch within the model — a sub-optimal choice. This new model structure to have more than  
650 one cohort for the same land cover within a grid cell, as has also been explored by Shevliakova et al.  
651 (2009) , will have impact on simulated biogeochemical and biophysical processes.

652

653 However, despite these improvements in model structure, it remains a big challenge to “seamlessly”  
654 integrate LUC forcing data into the model. The fundamental reason is that historical transitions of LUC  
655 are not reconstructed in a way being internally consistent with DGVMs. The systems to build historical  
656 LUC transitions (so-called land use models) and DGVMs may use different land cover types so that  
657 conciliating the two land cover maps is inevitable. This will lead to loss of information in incorporating  
658 forcing data into the model, as is also pointed out by Stocker et al. (2014). Second, simulated forest  
659 biomass density might be different as well, therefore the same amount of harvested wood volume may be  
660 translated into different forest areas in land use models and DGVMs. Recently progress has been made in  
661 DGVMs to represent forest stand structure and detailed management options (Naudts et al., 2015), so that  
662 harvested wood volume as a model output can be validated with statistical data. Third, the rotation length  
663 of shifting cultivation or forest management used in DGVMs may not be consistent with that assumed in  
664 land use models.

665

666 To overcome these obstacles and to promote a more comprehensive integration of LUC information into  
667 DGVMs, one possible route is to further develop DGVMs to partly embed functions of land use models.  
668 This will allow DGVMs to be used in an “inversed” manner than its current way of utilization. For  
669 example, food demand could be used as an input, so that dynamical decisions could be made within the  
670 model on how many croplands need to be created given the simulated crop yield by the crop module  
671 inside the DGVM. The same case also applies on pasture. Grassland management modules within  
672 DGVMs could generate information on meat and milk production etc., and this information could be used  
673 to inverse the meat and mild demand into demanded pasture areas (Chang et al., 2016). Harvested wood  
674 for a certain product usage might need wood with a specific diameter range, corresponding to a certain

675 forest age class given their simulated growth state, allowing the determination of both ages and areas of  
676 forests to be harvested.

677

## 678 **5 Conclusions**

679 In this study, we investigated the impacts on estimated historical gross land use change emissions by  
680 accounting for multiple sub-grid secondary land cohorts in a dynamic global vegetation model. The  
681 model employed here is capable of representing the rotation processes in land use and land management  
682 that mainly involve secondary forests, such as shifting cultivation and forest wood harvest.

683 Intermediately-aged secondary forests are given a high priority when forest clearing occurs in either  
684 shifting cultivation or wood harvest, complemented by older forests if young ones are insufficient to meet  
685 the prescribed land use transition. For the net LUC, clearing of forests starts exclusively from mature  
686 forests and move sequentially to younger forests when older ones are used up. This set of rules becomes  
687 indispensable when incorporating multiple sub-grid secondary land cohorts and reconciling with external  
688 land use transition forcing data in the model. As such, the simulated portfolio of secondary land cohorts  
689 within the model is driven by a reconstruction of historical gross land use change.

690

691 Following the input data of land use transition reconstruction, we assumed a constant shifting cultivation  
692 rotation length of 15 years in the tropics. We found that over 1501-2005, accounting for sub-grid  
693 secondary land cohorts yields a lower  $E_{LUC}$  than not (176 versus 197 Pg C), which is dominated by lower  
694 emissions from shifting cultivation (27 versus 46 Pg C or 40% lower in the former case). This is because  
695 secondary forests with a lower biomass are allowed being cleared, instead of the mature forests with a  
696 high biomass as in the approach to representing only mature forest in DGVMs. The lower emissions from  
697 shifting cultivation when accounting for sub-grid multiple land cohorts highly depend on the assumed  
698 rotation length. A set of sensitivity runs for Africa showed that a longer historical shifting cultivation  
699 rotation length leads to higher associated emissions. This highlights the need for more reliable  
700 reconstructions of the areas as well as the historical rotation lengths of shifting cultivation to reduce  
701 uncertainty on  $E_{LUC}$ . Our results show that although gross land use change as a previously neglected LUC  
702 emission component has been included by a growing number of DGVMs, its contribution to overall  $E_{LUC}$   
703 remains uncertain and tends to be overestimated by models ignoring sub-grid secondary forests.

704

## 705 **References:**

706 Amiro, B. D., Barr, A. G., Barr, J. G., Black, T. A., Bracho, R., Brown, M., Chen, J., Clark, K. L., Davis,  
707 K. J., Desai, A. R., Dore, S., Engel, V., Fuentes, J. D., Goldstein, A. H., Goulden, M. L., Kolb, T. E.,  
708 Lavigne, M. B., Law, B. E., Margolis, H. A., Martin, T., McCaughey, J. H., Misson, L., Montes-Helu,  
709 M., Noormets, A., Randerson, J. T., Starr, G. and Xiao, J.: Ecosystem carbon dioxide fluxes after

710 disturbance in forests of North America, *J. Geophys. Res.*, 115(G4), G00K02,  
711 doi:10.1029/2010JG001390, 2010.

712 Arneth, A., Sitch, S., Pongratz, J., Stocker, B. D., Ciais, P., Poulter, B., Bayer, A. D., Bondeau, A., Calle,  
713 L., Chini, L. P., Gasser, T., Fader, M., Friedlingstein, P., Kato, E., Li, W., Lindeskog, M., Nabel, J. E.  
714 M. S., Pugh, T. a. M., Robertson, E., Viovy, N., Yue, C. and Zaehle, S.: Historical carbon dioxide  
715 emissions caused by land-use changes are possibly larger than assumed, *Nature Geosci*, 10(2), 79–84,  
716 doi:10.1038/ngeo2882, 2017.

717 Avitabile, V., Herold, M., Heuvelink, G. B. M., Lewis, S. L., Phillips, O. L., Asner, G. P., Armston, J.,  
718 Ashton, P. S., Banin, L., Bayol, N., Berry, N. J., Boeckx, P., de Jong, B. H. J., DeVries, B., Girardin,  
719 C. A. J., Kearsley, E., Lindsell, J. A., Lopez-Gonzalez, G., Lucas, R., Malhi, Y., Morel, A., Mitchard,  
720 E. T. A., Nagy, L., Qie, L., Quinones, M. J., Ryan, C. M., Ferry, S. J. W., Sunderland, T., Laurin, G.  
721 V., Gatti, R. C., Valentini, R., Verbeeck, H., Wijaya, A. and Willcock, S.: An integrated pan-tropical  
722 biomass map using multiple reference datasets, *Glob Change Biol*, 22(4), 1406–1420,  
723 doi:10.1111/gcb.13139, 2016.

724 Baccini, A., Goetz, S. J., Walker, W. S., Laporte, N. T., Sun, M., Sulla-Menashe, D., Hackler, J., Beck, P.  
725 S. A., Dubayah, R., Friedl, M. A., Samanta, S. and Houghton, R. A.: Estimated carbon dioxide  
726 emissions from tropical deforestation improved by carbon-density maps, *Nature Clim. Change*, 2(3),  
727 182–185, doi:10.1038/nclimate1354, 2012.

728 Bayer, A. D., Lindeskog, M., Pugh, T. A. M., Anthoni, P. M., Fuchs, R. and Arneth, A.: Uncertainties in  
729 the land-use flux resulting from land-use change reconstructions and gross land transitions, *Earth*  
730 *Syst. Dynam.*, 8(1), 91–111, doi:10.5194/esd-8-91-2017, 2017.

731 Chang, J., Ciais, P., Herrero, M., Havlik, P., Campioli, M., Zhang, X., Bai, Y., Viovy, N., Joiner, J.,  
732 Wang, X., Peng, S., Yue, C., Piao, S., Wang, T., Hauglustaine, D. A., Soussana, J.-F., Peregon, A.,  
733 Kosykh, N. and Mironycheva-Tokareva, N.: Combining livestock production information in a  
734 process-based vegetation model to reconstruct the history of grassland management, *Biogeosciences*,  
735 13(12), 3757–3776, doi:10.5194/bg-13-3757-2016, 2016.

736 Chazdon, R. L., Broadbent, E. N., Rozendaal, D. M. A., Bongers, F., Zambrano, A. M. A., Aide, T. M.,  
737 Balvanera, P., Becknell, J. M., Boukili, V., Brancalion, P. H. S., Craven, D., Almeida-Cortez, J. S.,  
738 Cabral, G. A. L., Jong, B. de, Denslow, J. S., Dent, D. H., DeWalt, S. J., Dupuy, J. M., Durán, S. M.,  
739 Espirito-Santo, M. M., Fandino, M. C., César, R. G., Hall, J. S., Hernández-Stefanoni, J. L., Jakovac,  
740 C. C., Junqueira, A. B., Kennard, D., Letcher, S. G., Lohbeck, M., Martínez-Ramos, M., Massoca, P.,  
741 Meave, J. A., Mesquita, R., Mora, F., Muñoz, R., Muscarella, R., Nunes, Y. R. F., Ochoa-Gaona, S.,  
742 Orihuela-Belmonte, E., Peña-Claros, M., Pérez-García, E. A., Piotto, D., Powers, J. S., Rodríguez-  
743 Velazquez, J., Romero-Pérez, I. E., Ruíz, J., Saldarriaga, J. G., Sanchez-Azofeifa, A., Schwartz, N.  
744 B., Steininger, M. K., Swenson, N. G., Uriarte, M., Breugel, M. van, Wal, H. van der, Veloso, M. D.  
745 M., Vester, H., Vieira, I. C. G., Bentos, T. V., Williamson, G. B. and Poorter, L.: Carbon  
746 sequestration potential of second-growth forest regeneration in the Latin American tropics, *Science*  
747 *Advances*, 2(5), e1501639, doi:10.1126/sciadv.1501639, 2016.

748 Don, A., Schumacher, J. and Freibauer, A.: Impact of tropical land-use change on soil organic carbon  
749 stocks – a meta-analysis, *Global Change Biology*, 17(4), 1658–1670, doi:10.1111/j.1365-  
750 2486.2010.02336.x, 2011.

751 Erb, K.-H., Luysaert, S., Meyfroidt, P., Pongratz, J., Don, A., Kloster, S., Kuemmerle, T., Fetzel, T.,  
752 Fuchs, R., Herold, M., Haberl, H., Jones, C. D., Marín-Spiotta, E., McCallum, I., Robertson, E.,  
753 Seufert, V., Fritz, S., Valade, A., Wiltshire, A. and Dolman, A. J.: Land management: data availability

754 and process understanding for global change studies, *Glob Change Biol*, 23(2), 512–533,  
755 doi:10.1111/gcb.13443, 2017.

756 Gasser, T. and Ciais, P.: A theoretical framework for the net land-to-atmosphere CO<sub>2</sub> flux and its  
757 implications in the definition of “emissions from land-use change,” *Earth Syst. Dynam.*, 4(1), 171–  
758 186, doi:10.5194/esd-4-171-2013, 2013.

759 Guimberteau, M., Zhu, D., Maignan, F., Huang, Y., Yue, C., Dantec-Nédélec, S., Ottlé, C., Jornet-Puig,  
760 A., Bastos, A., Laurent, P., Goll, D., Bowring, S., Chang, J., Guenet, B., Tifafi, M., Peng, S., Krinner,  
761 G., Ducharne, A., Wang, F., Wang, T., Wang, X., Wang, Y., Yin, Z., Lauerwald, R., Joetzer, E., Qiu,  
762 C., Kim, H. and Ciais, P.: ORCHIDEE-MICT (v8.4.1), a land surface model for the high latitudes:  
763 model description and validation, *Geosci. Model Dev.*, 11(1), 121–163, doi:10.5194/gmd-11-121-  
764 2018, 2018.

765 Hansis, E., Davis, S. J. and Pongratz, J.: Relevance of methodological choices for accounting of land use  
766 change carbon fluxes, *Global Biogeochem. Cycles*, 29(8), 2014GB004997,  
767 doi:10.1002/2014GB004997, 2015.

768 Houghton, R. A.: The annual net flux of carbon to the atmosphere from changes in land use 1850–1990\*,  
769 *Tellus B*, 51(2), 298–313, doi:10.1034/j.1600-0889.1999.00013.x, 1999.

770 Houghton, R. A.: Revised estimates of the annual net flux of carbon to the atmosphere from changes in  
771 land use and land management 1850–2000, *Tellus B*, 55(2), 378–390, doi:10.1034/j.1600-  
772 0889.2003.01450.x, 2003.

773 Houghton, R. A.: How well do we know the flux of CO<sub>2</sub> from land-use change?, *Tellus B*, 62(5), 337–  
774 351, doi:10.1111/j.1600-0889.2010.00473.x, 2010.

775 Houghton, R. A. and Nassikas, A. A.: Global and regional fluxes of carbon from land use and land cover  
776 change 1850–2015, *Global Biogeochem. Cycles*, 31(3), 2016GB005546,  
777 doi:10.1002/2016GB005546, 2017.

778 Hurtt, G. C., Chini, L. P., Frolking, S., Betts, R. A., Feddema, J., Fischer, G., Fisk, J. P., Hibbard, K.,  
779 Houghton, R. A., Janetos, A., Jones, C. D., Kindermann, G., Kinoshita, T., Goldewijk, K. K., Riahi,  
780 K., Shevliakova, E., Smith, S., Stehfest, E., Thomson, A., Thornton, P., Vuuren, D. P. van and Wang,  
781 Y. P.: Harmonization of land-use scenarios for the period 1500–2100: 600 years of global gridded  
782 annual land-use transitions, wood harvest, and resulting secondary lands, *Climatic Change*, 109(1–2),  
783 117, doi:10.1007/s10584-011-0153-2, 2011.

784 Kato, E., Kinoshita, T., Ito, A., Kawamiya, M. and Yamagata, Y.: Evaluation of spatially explicit  
785 emission scenario of land-use change and biomass burning using a process-based biogeochemical  
786 model, *Journal of Land Use Science*, 8(1), 104–122, doi:10.1080/1747423X.2011.628705, 2013.

787 Krinner, G., Viovy, N., de Noblet-Ducoudré, N., Ogée, J., Polcher, J., Friedlingstein, P., Ciais, P., Sitch,  
788 S. and Prentice, I. C.: A dynamic global vegetation model for studies of the coupled atmosphere-  
789 biosphere system, *Global Biogeochemical Cycles*, 19(1), GB1015, doi:10.1029/2003GB002199,  
790 2005.

791 Le Quéré, C., Andrew, R. M., Canadell, J. G., Sitch, S., Korsbakken, J. I., Peters, G. P., Manning, A. C.,  
792 Boden, T. A., Tans, P. P., Houghton, R. A., Keeling, R. F., Alin, S., Andrews, O. D., Anthoni, P.,  
793 Barbero, L., Bopp, L., Chevallier, F., Chini, L. P., Ciais, P., Currie, K., Delire, C., Doney, S. C.,  
794 Friedlingstein, P., Gkritzalis, T., Harris, I., Hauck, J., Haverd, V., Hoppema, M., Klein Goldewijk, K.,  
795 Jain, A. K., Kato, E., Körtzinger, A., Landschützer, P., Lefèvre, N., Lenton, A., Lienert, S.,  
796 Lombardozzi, D., Melton, J. R., Metzl, N., Millero, F., Monteiro, P. M. S., Munro, D. R., Nabel, J. E.  
797 M. S., Nakaoka, S., O’Brien, K., Olsen, A., Omar, A. M., Ono, T., Pierrot, D., Poulter, B.,

798 Rödenbeck, C., Salisbury, J., Schuster, U., Schwinger, J., Séférian, R., Skjelvan, I., Stocker, B. D.,  
799 Sutton, A. J., Takahashi, T., Tian, H., Tilbrook, B., Laan-Luijkx, I. T. van der, Werf, G. R. van der,  
800 Viovy, N., Walker, A. P., Wiltshire, A. J. and Zaehle, S.: Global Carbon Budget 2016, *Earth System*  
801 *Science Data*, 8(2), 605–649, doi:10.5194/essd-8-605-2016, 2016.

802 Li, W., MacBean, N., Ciais, P., Defourny, P., Lamarche, C., Bontemps, S., Houghton, R. A. and Peng, S.:  
803 Gross and net land cover changes based on plant functional types derived from the annual ESA CCI  
804 land cover maps, *Earth System Science Data Discussions*, 1–23, doi:https://doi.org/10.5194/essd-  
805 2017-74, 2017a.

806 Li, W., Ciais, P., Peng, S., Yue, C., Wang, Y., Thurner, M., Saatchi, S. S., Arneeth, A., Avitabile, V.,  
807 Carvalhais, N., Harper, A. B., Kato, E., Koven, C., Liu, Y. Y., Nabel, J. E. M. S., Pan, Y., Pongratz,  
808 J., Poulter, B., Pugh, T. A. M., Santoro, M., Sitch, S., Stocker, B. D., Viovy, N., Wiltshire, A.,  
809 Yousefpour, R. and Zaehle, S.: Land-use and land-cover change carbon emissions between 1901 and  
810 2012 constrained by biomass observations, *Biogeosciences Discuss.*, 2017, 1–25, doi:10.5194/bg-  
811 2017-186, 2017b.

812 Luysaert, S., Jammert, M., Stoy, P. C., Estel, S., Pongratz, J., Ceschia, E., Churkina, G., Don, A., Erb, K.,  
813 Ferlicoq, M., Gielen, B., Grünwald, T., Houghton, R. A., Klumpp, K., Knohl, A., Kolb, T.,  
814 Kuemmerle, T., Laurila, T., Lohila, A., Loustau, D., McGrath, M. J., Meyfroidt, P., Moors, E. J.,  
815 Naudts, K., Novick, K., Otto, J., Pilegaard, K., Pio, C. A., Rambal, S., Rebmann, C., Ryder, J.,  
816 Suyker, A. E., Varlagin, A., Wattenbach, M. and Dolman, A. J.: Land management and land-cover  
817 change have impacts of similar magnitude on surface temperature, *Nature Clim. Change*, 4(5), 389–  
818 393, doi:10.1038/nclimate2196, 2014.

819 McGrath, M. J., Luysaert, S., Meyfroidt, P., Kaplan, J. O., Bürgi, M., Chen, Y., Erb, K., Gimmi, U.,  
820 McInerney, D., Naudts, K., Otto, J., Pasztor, F., Ryder, J., Schelhaas, M.-J. and Valade, A.:  
821 Reconstructing European forest management from 1600 to 2010, *Biogeosciences*, 12(14), 4291–4316,  
822 doi:10.5194/bg-12-4291-2015, 2015.

823 Meiyappan, P. and Jain, A. K.: Three distinct global estimates of historical land-cover change and land-  
824 use conversions for over 200 years, *Front. Earth Sci.*, 6(2), 122–139, doi:10.1007/s11707-012-0314-2,  
825 2012.

826 Naudts, K., Ryder, J., McGrath, M. J., Otto, J., Chen, Y., Valade, A., Bellasen, V., Berhongaray, G.,  
827 Bönisch, G., Campioli, M., Ghattas, J., De Groote, T., Haverd, V., Kattge, J., MacBean, N., Maignan,  
828 F., Merilä, P., Penuelas, J., Peylin, P., Pinty, B., Pretzsch, H., Schulze, E. D., Solyga, D., Vuichard,  
829 N., Yan, Y. and Luysaert, S.: A vertically discretised canopy description for ORCHIDEE (SVN  
830 r2290) and the modifications to the energy, water and carbon fluxes, *Geosci. Model Dev.*, 8(7),  
831 2035–2065, doi:10.5194/gmd-8-2035-2015, 2015.

832 Pan, Y., Chen, J. M., Birdsey, R., McCullough, K., He, L. and Deng, F.: Age structure and disturbance  
833 legacy of North American forests, *Biogeosciences*, 8(3), 715–732, doi:10.5194/bg-8-715-2011, 2011.

834 Peng, S., Ciais, P., Maignan, F., Li, W., Chang, J., Wang, T. and Yue, C.: Sensitivity of land use change  
835 emission estimates to historical land use and land cover mapping, *Global Biogeochem. Cycles*, 31(4),  
836 2015GB005360, doi:10.1002/2015GB005360, 2017.

837 Piao, S., Ciais, P., Friedlingstein, P., de Noblet-Ducoudré, N., Cadule, P., Viovy, N. and Wang, T.:  
838 Spatiotemporal patterns of terrestrial carbon cycle during the 20th century, *Global Biogeochem.*  
839 *Cycles*, 23(4), GB4026, doi:10.1029/2008GB003339, 2009a.

840 Piao, S., Fang, J., Ciais, P., Peylin, P., Huang, Y., Sitch, S. and Wang, T.: The carbon balance of  
841 terrestrial ecosystems in China, *Nature*, 458(7241), 1009–1013, doi:10.1038/nature07944, 2009b.



842 Poeplau, C., Don, A., Vesterdal, L., Leifeld, J., Van Wesemael, B., Schumacher, J. and Gensior, A.:  
843 Temporal dynamics of soil organic carbon after land-use change in the temperate zone – carbon  
844 response functions as a model approach, *Global Change Biology*, 17(7), 2415–2427,  
845 doi:10.1111/j.1365-2486.2011.02408.x, 2011.

846 Pongratz, J., Reick, C. H., Raddatz, T. and Claussen, M.: Effects of anthropogenic land cover change on  
847 the carbon cycle of the last millennium, *Global Biogeochem. Cycles*, 23(4), GB4001,  
848 doi:10.1029/2009GB003488, 2009.

849 Poorter, L., Bongers, F., Aide, T. M., Almeyda Zambrano, A. M., Balvanera, P., Becknell, J. M., Boukili,  
850 V., Brancalion, P. H. S., Broadbent, E. N., Chazdon, R. L., Craven, D., de Almeida-Cortez, J. S.,  
851 Cabral, G. A. L., de Jong, B. H. J., Denslow, J. S., Dent, D. H., DeWalt, S. J., Dupuy, J. M., Durán, S.  
852 M., Espírito-Santo, M. M., Fandino, M. C., César, R. G., Hall, J. S., Hernandez-Stefanoni, J. L.,  
853 Jakovac, C. C., Junqueira, A. B., Kennard, D., Letcher, S. G., Licona, J.-C., Lohbeck, M., Marín-  
854 Spiotta, E., Martínez-Ramos, M., Massoca, P., Meave, J. A., Mesquita, R., Mora, F., Muñoz, R.,  
855 Muscarella, R., Nunes, Y. R. F., Ochoa-Gaona, S., de Oliveira, A. A., Orihuela-Belmonte, E., Peña-  
856 Claros, M., Pérez-García, E. A., Piotta, D., Powers, J. S., Rodríguez-Velázquez, J., Romero-Pérez, I.  
857 E., Ruíz, J., Saldarriaga, J. G., Sanchez-Azofeifa, A., Schwartz, N. B., Steininger, M. K., Swenson, N.  
858 G., Toledo, M., Uriarte, M., van Breugel, M., van der Wal, H., Veloso, M. D. M., Vester, H. F. M.,  
859 Vicentini, A., Vieira, I. C. G., Bentos, T. V., Williamson, G. B. and Rozendaal, D. M. A.: Biomass  
860 resilience of Neotropical secondary forests, *Nature*, 530(7589), 211–214, doi:10.1038/nature16512,  
861 2016.

862 Saatchi, S. S., Harris, N. L., Brown, S., Lefsky, M., Mitchard, E. T. A., Salas, W., Zutta, B. R.,  
863 Buermann, W., Lewis, S. L., Hagen, S., Petrova, S., White, L., Silman, M. and Morel, A.: Benchmark  
864 map of forest carbon stocks in tropical regions across three continents, *PNAS*,  
865 doi:10.1073/pnas.1019576108, 2011.

866 Santoro, M., Beaudoin, A., Beer, C., Cartus, O., Fransson, J. E. S., Hall, R. J., Pathe, C., Schmillius, C.,  
867 Schepaschenko, D., Shvidenko, A., Thurner, M. and Wegmüller, U.: Forest growing stock volume of  
868 the northern hemisphere: Spatially explicit estimates for 2010 derived from Envisat ASAR, *Remote  
869 Sensing of Environment*, 168, 316–334, doi:10.1016/j.rse.2015.07.005, 2015.

870 Shevliakova, E., Pacala, S. W., Malyshev, S., Hurtt, G. C., Milly, P. C. D., Caspersen, J. P., Sentman, L.  
871 T., Fisk, J. P., Wirth, C. and Crevoisier, C.: Carbon cycling under 300 years of land use change:  
872 Importance of the secondary vegetation sink, *Global Biogeochem. Cycles*, 23(2), GB2022,  
873 doi:10.1029/2007GB003176, 2009.

874 Smith, B., Prentice, I. C. and Sykes, M. T.: Representation of vegetation dynamics in the modelling of  
875 terrestrial ecosystems: comparing two contrasting approaches within European climate space, *Global  
876 Ecology and Biogeography*, 10(6), 621–637, doi:10.1046/j.1466-822X.2001.t01-1-00256.x, 2001.

877 Stocker, B. D., Feissli, F., Strassmann, K. M., Spahni, R. and Joos, F.: Past and future carbon fluxes from  
878 land use change, shifting cultivation and wood harvest, *Tellus B*, 66(0),  
879 doi:10.3402/tellusb.v66.23188, 2014.

880 van Vliet, N., Mertz, O., Heinimann, A., Langanke, T., Pascual, U., Schmook, B., Adams, C., Schmidt-  
881 Vogt, D., Messerli, P., Leisz, S., Castella, J.-C., Jørgensen, L., Birch-Thomsen, T., Hett, C., Bech-  
882 Bruun, T., Ickowitz, A., Vu, K. C., Yasuyuki, K., Fox, J., Padoch, C., Dressler, W. and Ziegler, A. D.:  
883 Trends, drivers and impacts of changes in swidden cultivation in tropical forest-agriculture frontiers:  
884 A global assessment, *Global Environmental Change*, 22(2), 418–429,  
885 doi:10.1016/j.gloenvcha.2011.10.009, 2012.

886 van der Werf, G. R., Randerson, J. T., Giglio, L., Collatz, G. J., Mu, M., Kasibhatla, P. S., Morton, D. C.,  
887 DeFries, R. S., Jin, Y. and van Leeuwen, T. T.: Global fire emissions and the contribution of  
888 deforestation, savanna, forest, agricultural, and peat fires (1997–2009), *Atmos. Chem. Phys.*, 10(23),  
889 11707–11735, doi:10.5194/acp-10-11707-2010, 2010.  
890 Wilkenskjeld, S., Kloster, S., Pongratz, J., Raddatz, T. and Reick, C. H.: Comparing the influence of net  
891 and gross anthropogenic land-use and land-cover changes on the carbon cycle in the MPI-ESM,  
892 *Biogeosciences*, 11(17), 4817–4828, doi:10.5194/bg-11-4817-2014, 2014.  
893 Yang, X., Richardson, T. K. and Jain, A. K.: Contributions of secondary forest and nitrogen dynamics to  
894 terrestrial carbon uptake, *Biogeosciences*, 7(10), 3041–3050, doi:10.5194/bg-7-3041-2010, 2010.  
895 Yue, C., Ciais, P., Cadule, P., Thonicke, K., Archibald, S., Poulter, B., Hao, W. M., Hantson, S.,  
896 Mouillot, F., Friedlingstein, P., Maignan, F. and Viovy, N.: Modelling the role of fires in the  
897 terrestrial carbon balance by incorporating SPITFIRE into the global vegetation model ORCHIDEE –  
898 Part 1: simulating historical global burned area and fire regimes, *Geosci. Model Dev.*, 7(6), 2747–  
899 2767, doi:10.5194/gmd-7-2747-2014, 2014.  
900 Yue, C., Ciais, P., Luyssaert, S., Li, W., McGrath, M. J., Chang, J. and Peng, S.: Representing  
901 anthropogenic gross land use change, wood harvest and forest age dynamics in a global vegetation  
902 model ORCHIDEE-MICT (r4259), *Geosci. Model Dev. Discuss.*, 2017, 1–38, doi:10.5194/gmd-  
903 2017-118, 2017.

904

#### 905 **Data availability**

906 All data used to generate the figures are available upon the request to the corresponding author.

#### 907 **Competing interests**

908 The authors declare that they have no conflict of interest.

909

#### 910 **Acknowledgments**

911 C.Y., P.C. and W.L. acknowledge support from the European Research Council through Synergy grant  
912 ERC-2013-SyG-610028 “IMBALANCE-P”. W.L. and C.Y. are also supported by the European  
913 Commission-funded project LUC4C (No. 603542). The authors thank the two reviewers for their  
914 constructive comments that help to improve the manuscript quality.

915

916 **Tables and figures**

917 Table 1 Factorial simulations to quantify  $E_{LUC}$  from each of the LUC processes considered: net land use  
 918 change ( $E_{LUC\ net}$ ), land turnover ( $E_{LUC\ turnover}$ ) and wood harvest ( $E_{LUC\ harvest}$ ), with  $E_{LUC\ all}$  being carbon  
 919 emissions from all the three processes. The plus sign (“+”) indicate that the process in question is  
 920 included, with  $S0_{ageless}$  ( $S0_{age}$ ) having no LUC activities to  $S3_{ageless}$  ( $S3_{age}$ ) including all LUC processes.  
 921  $E_{LUC}$  is quantified as the difference in net biome production (NBP) between simulations without and with  
 922 LUC. To explore the uncertainties by using a fully additive approach, we included an alternative S2b  
 923 simulation, which includes net land use change and land turnover.  $E_{LUC\ turnover}$  and  $E_{LUC\ harvest}$  are  
 924 consequently calculated using this alternative simulation as well.

<b>Simulations and LUC processes included</b>			
Simulations	Net land use change	Land turnover	Wood harvest
$S0_{ageless}$ ( $S0_{age}$ )			
$S1_{ageless}$ ( $S1_{age}$ )	+		
$S2_{ageless}$ ( $S2_{age}$ )	+	+	
$S3_{ageless}$ ( $S3_{age}$ )	+	+	+
$S2b_{ageless}$ ( $S2b_{age}$ )	+		+
<b>Calculation of <math>E_{LUC}</math></b>			
No age dynamics ( $S_{ageless}$ )		With age dynamics ( $S_{age}$ )	
$E_{LUC\ net, ageless} = NBP_{S0, ageless} - NBP_{S1, ageless}$		$E_{LUC\ net, age} = NBP_{S0, age} - NBP_{S1, age}$	
$E_{LUC\ turnover, ageless} = NBP_{S1, ageless} - NBP_{S2, ageless}$		$E_{LUC\ turnover, age} = NBP_{S1, age} - NBP_{S2, age}$	
$E_{LUC\ harvest, ageless} = NBP_{S2, ageless} - NBP_{S3, ageless}$		$E_{LUC\ harvest, age} = NBP_{S2, age} - NBP_{S3, age}$	
$E_{LUC\ turnover, ageless\ S2b} = NBP_{S2b, ageless} - NBP_{S3, ageless}$		$*E_{LUC\ turnover, age\ S2b} = NBP_{S2b, age} - NBP_{S3, age}$	
$E_{LUC\ harvest, ageless\ S2b} = NBP_{S1, ageless} - NBP_{S2b, ageless}$		$*E_{LUC\ harvest, age\ S2b} = NBP_{S1, age} - NBP_{S2b, age}$	
$E_{LUC\ all, ageless} = NBP_{S0, ageless} - NBP_{S3, ageless}$		$E_{LUC\ all, age} = NBP_{S0, age} - NBP_{S3, age}$	

925

926 Table 2 Determination of woody biomass thresholds for different age classes of forest PFTs. We first look  
 927 up through the biomass-age curve (Eq. 2) for a ratio of woody biomass to the maximum biomass that  
 928 correspond to certain ages (years), and then multiply this ratio with equilibrium biomass at the end of  
 929 spin-up for each grid cell. Numbers in the table indicate the ratio of woody biomass to the maximum  
 930 woody biomass ( $B_{max}$  in Eq. 2), and the numbers in parentheses indicate the corresponding forest age.

Forest cohorts	Tropical forest	Temperate forest	Boreal forest
Age1	0.1 (3 year)	0.07 (3 year)	0.04 (3 year)
Age2	0.26 (9 year)	0.22 (10 year)	0.19 (15 year)
Age3	0.39 (15 year)	0.40 (20 year)	0.34 (30 year)
Age4	0.6 (27 year)	0.6 (35 year)	0.6 (65 year)
Age5	0.8 (48 year)	0.8 (64 year)	0.8 (114 year)
Age6	1.2 (>48 year)	1.2 (>64 year)	1.2 (>114 year)

931  
 932 Table 3 Cumulative  $E_{LUC}$  for 1501–2005 (Pg C) from different processes quantified by different  
 933 approaches (see Table 1 for detailed calculations of various  $E_{LUC}$ ).

	No age dynamics	With age dynamics	Emission change in $S_{age}$ relative to $S_{ageless}$ (%)
$E_{LUC\ net}$	123.7	118.0	-4.6%
$E_{LUC\ turnover}$	45.4	27.3	-40%
$E_{LUC\ turnover\ S2b}$	39.9	25.1	-37%
$E_{LUC\ harvest}$	27.4	30.8	12%
$E_{LUC\ harvest\ S2b}$	32.9	33.0	0.0%
$E_{LUC\ all}$	196.5	176.1	10%

934  
 935 Table 4 Carbon emissions from gross and net land use transitions, contributions of gross transitions to the  
 936 total emissions from different studies, adapted from Hansis et al. (2015).

Reference	Time period	$E_{LUC}$ (Pg C)		Contribution of gross transitions, Pg C (%) <sup>d</sup>
		Gross transitions	Net transitions	
This study ( $S_{age}$ )	1850-2005	147	99	22 (15%)
This study ( $S_{ageless}$ )	1850-2005	158	104	31(20%)
Hansis et al. (2015) <sup>a</sup>	1500–2012	382	374	8.5 (2%)

Hansis et al. (2015) <sup>b</sup>	1500–2012	382	290	92.4 (24%)
Hansis et al. (2015) <sup>c</sup>	1500–2012	382	296	85.8 (22%)
Stocker et al. (2014)	1850–2004	171	146	25 (15%)
Wilkenskjeld et al. (2014)	1850–2005	225	140	85 (38%)
Houghton (2010)	1850–2005	156		(28%, tropics)

937 <sup>a</sup> Only secondary land is cleared in gross transitions. <sup>b</sup> Primary land is first cleared in gross transitions. <sup>c</sup>

938 Primary land is last cleared in gross transitions. <sup>d</sup> The last column gives the difference in  $E_{LUC}$  between

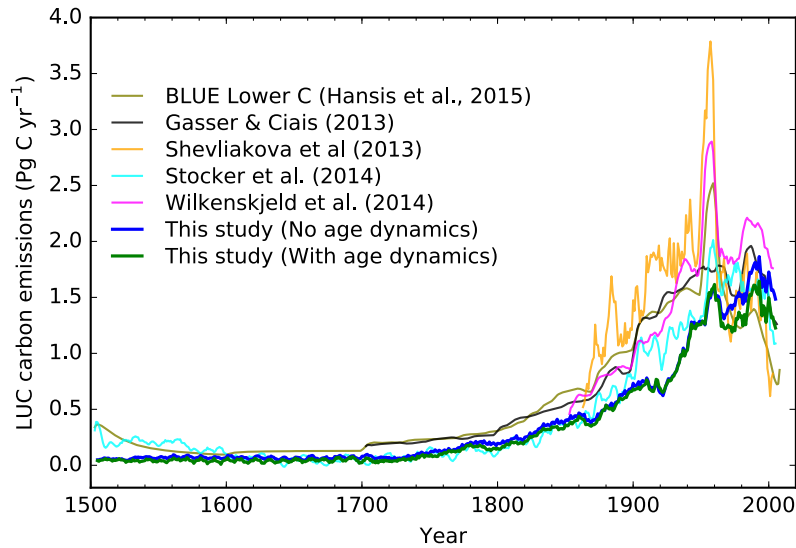
939 gross and net transitions (the absolute value in Pg C and relative to the net  $E_{LUC}$ ).

940

941

942

943

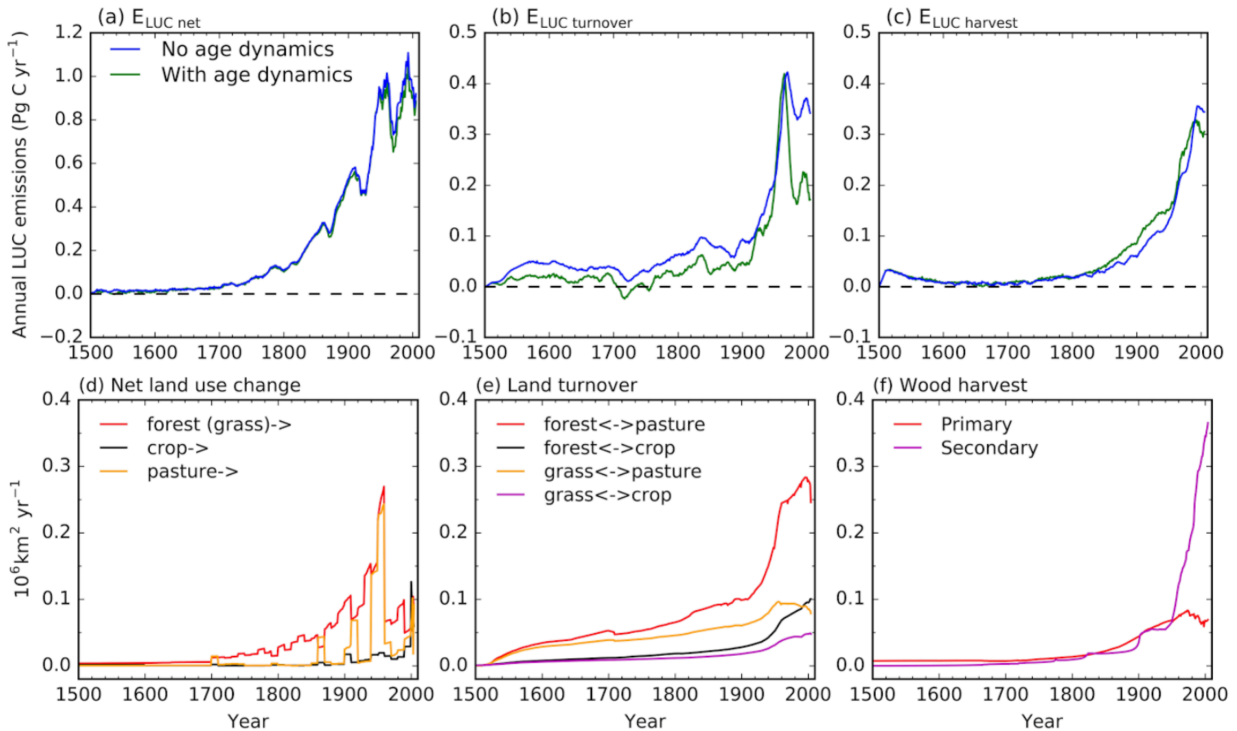


944

945 Fig. 1 Annual carbon emissions from historical land use change over the globe by our studies and from  
 946 other previous studies. Results of this study are smoothed using a ten-year average moving window; data  
 947 of other studies are from Figure 5 Hansis et al. (2015) and are smoothed using a five-year moving average  
 948 window.

949

950

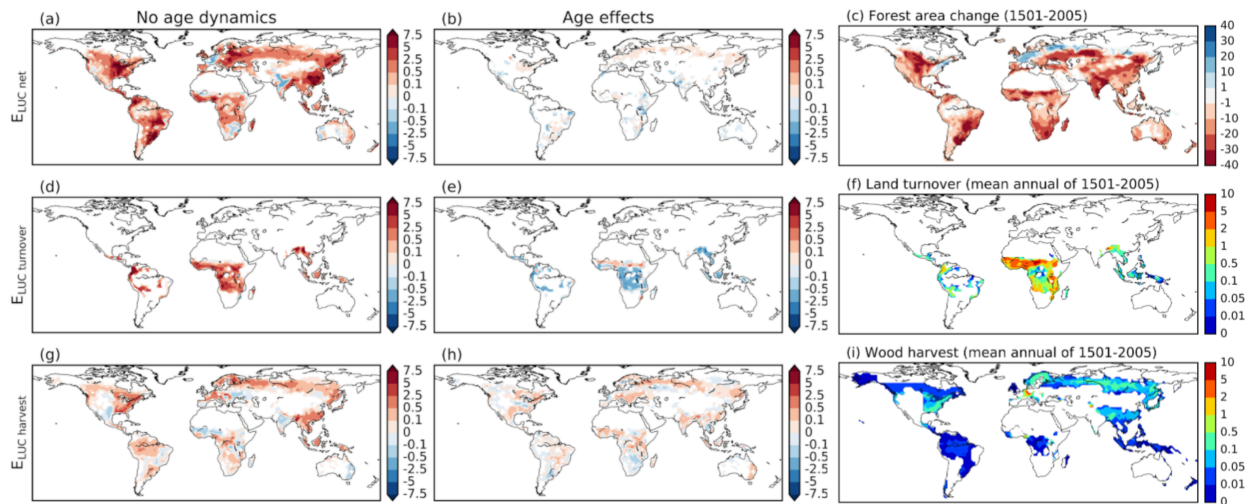


951

952 Fig. 2 Upper panels: annual carbon emissions since 1501 from different LUC processes, (a) net land use  
 953 change, (b) land turnover and (c) wood harvest. Data are smoothed using a ten-year average moving  
 954 window. Lower panels: annual time series of areas impacted by different LUC processes. (d) Area losses  
 955 of forest, grassland, cropland and pasture as a result of net land use change. Note that we assume equal  
 956 contributions by forest and grassland to agricultural land when backcasting historical land cover maps,  
 957 thus area losses of forest and grassland are identical. (e) Areas subject to land turnover. (f) Areas of wood  
 958 harvest from primary and secondary forests.

959

960

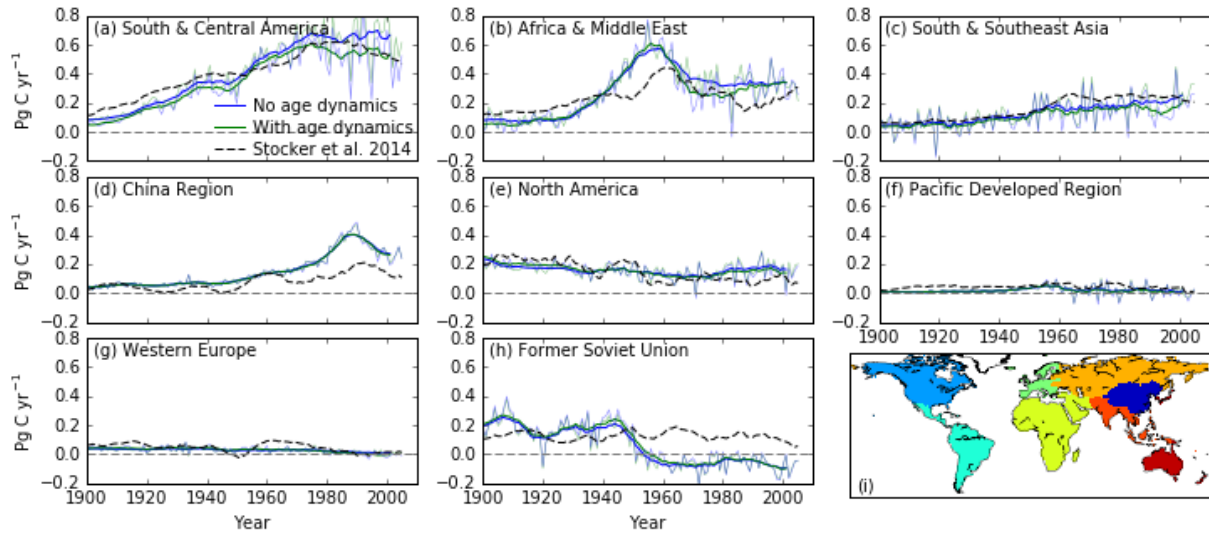


961

962 Fig. 3 (a)–(c): Spatial distribution of  $E_{LUC\ net}$  for 1501–2005 ( $\text{kg C m}^{-2}$ ) as simulated by  $S_{ageless}$  simulations,  
 963 the age effect quantified as difference in  $E_{LUC\ net}$  between  $S_{age}$  and  $S_{ageless}$ , and the cumulative forest loss as  
 964 a result of net land use change as a percentage of grid cell area. (d)–(f): similar as (a)–(c) but for  $E_{LUC}$   
 965 turnover, with (f) showing the mean annual grid cell percentage impacted by land turnover over 1501–2005.  
 966 (g)–(i) similar as (a)–(c) but for  $E_{LUC\ harvest}$ , with (i) showing the mean annual grid cell percentage  
 967 impacted by wood harvest (i.e., sum of wood harvest on primary and secondary forests) over 1501–2005.

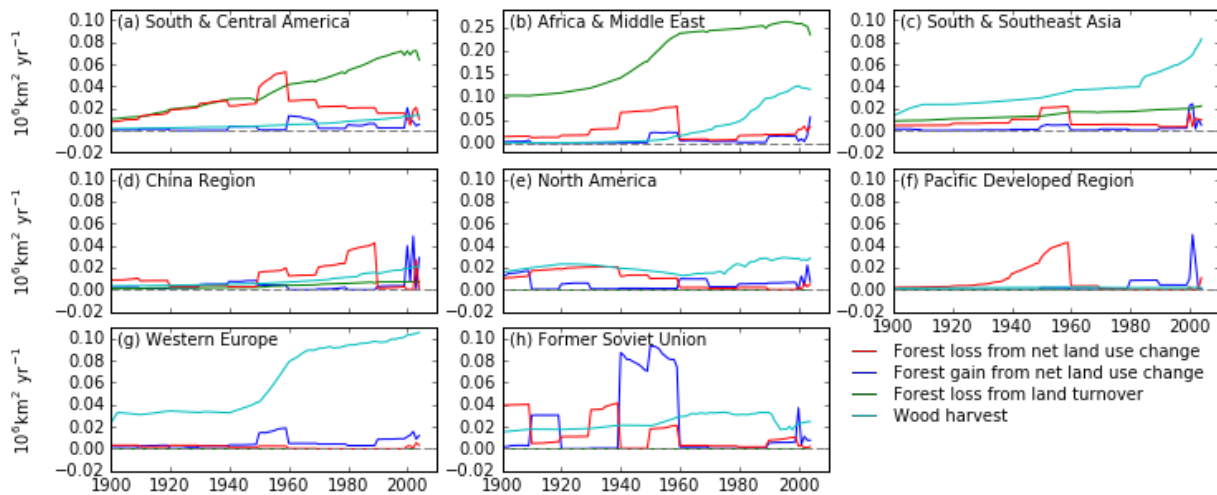
968

969



970 Fig. 4 (a)-(h) Temporal patterns of regional land use change emissions in comparison with those from  
 971 Stocker et al. (2014). Thicker solid lines indicate smoothed annual emissions by ten-year moving average  
 972 from our study, with blue (green) showing emissions from  $S_{ageless}$  ( $S_{age}$ ) simulations. Thinner solid lines  
 973 indicate unsmoothed annual emissions from our study. Gray dashed lines indicate estimations from  
 974 Stocker et al. (2014), smoothed by ten-year moving average. Regional segregation of the globe is shown  
 975 in the subplot (i).  
 976

977  
 978



979 Fig. 5 Annual regional areas subject to land use change. Only land use change activities involving forests  
 980 are assumed to have dominant impacts on  $E_{LUC}$  and are thus shown here: forest loss (red line) and gain  
 981 (blue line) from net land use change, occurring within the same region but not in the same model grid  
 982 cell; forest involved in land turnover (green line) and wood harvest (cyan line), where forested land  
 983



984 remain a forest after land use change. Note that the scale of y-axis is the subplot (b) is different from the  
985 others. See Fig. 4 for the spatial extents of different regions.